



Contents lists available at ScienceDirect

Saudi Journal of Biological Sciences

journal homepage: www.sciencedirect.com



Original article

A comparative *ex vivo* permeation evaluation of a novel 5-Fluorouracil nanoemulsion-gel by topically applied in the different excised rat, goat, and cow skinNiyaz Ahmad^{a,b,*}, Rizwan Ahmad^c, Taysser Mohammed Buhezaha^a, Hussain Salman AlHomoud^a, Hassan Ali Al-Nasif^a, Md Sarafroz^b^aDepartment of Pharmaceutics, College of Clinical Pharmacy, Imam Abdulrahman Bin Faisal University, Dammam, Saudi Arabia^bDepartment of Pharmaceutical Chemistry, College of Clinical Pharmacy, Imam Abdulrahman Bin Faisal University, Dammam, Saudi Arabia^cDepartment of Natural Products and Alternative Medicine, College of Clinical Pharmacy, Imam Abdulrahman Bin Faisal University, Dammam, Saudi Arabia

ARTICLE INFO

Article history:

Received 22 December 2019

Revised 13 February 2020

Accepted 24 February 2020

Available online 3 March 2020

Keywords:

5-Fluorouracil

Nanoemulsion

Nanoemulsion-gel

Different skin permeation,

chemoprevention

Cytotoxic activity

Local accumulation efficiency

Transdermal delivery

ABSTRACT

Aim of the study: 5-Fluorouracil (5-FU) can't be given orally because of very low bioavailability and produces serious adverse effects. Therefore, the main objective of this research is to develop, evaluate, and comparative effects by different nanoformulations of topical application on chemoprevention of skin cancer in different types of skin.

Material and methods: Castor oil (oil), Transcutol HP (surfactant), and Polyethylene glycol (PEG)-400 (co-surfactant) have taken on the basis of nonionic property and highest nanoemulsion (NE)-region. Aqueous micro titration method with ultra-sonication method (based on high energy) was used for the preparation of 5-FU-NE. Optimized-5-FU-NE was stable thermodynamically, and their characterizations was performed on the basis of globule size, zeta potential, refractive index, and viscosity. Optimized-NE has been converted into 5-FU-NE-Gel with the help of Carbopol® 934 and also performed their permeation studies in the different skins (cow, goat, and rat, *ex vivo*) using Logan transdermal diffusion cell (DHC-6T). Optimized-5-FU-NE and 5-FU-NE-Gel were evaluated cytotoxic studies (*in vitro*) on the melanoma cell lines.

Results: The permeation of 5-FU from 5-FU-NE-Gel nanoformulation for rat skin model was 1.56 times higher than the 5-FU-NE and 12.51 times higher than the 5-FU-S for the cow and goat skin model. The values of steady state flux and permeability coefficient for 5-FU-NE-Gel of rat skin were higher i.e. $12.0244 \pm 1.12 \mu\text{g cm}^{-2}\text{h}^{-1}$ and $1.2024 \pm 0.073 \times 10^{-2} \mu\text{g cm}^{-2}\text{h}^{-1}$, respectively. Optimized-5-FU-NE and 5-FU-NE-Gel nanoformulation were found to be physically stable. SK-MEL-5 cancer cells have showed the results based on cytotoxicity studies (*in vitro*) that 5-FU as Optimized-5-FU-NE-Gel is much more efficacious than 5-FU-NE followed by free 5-FU. Localization of 5-FU from 5-FU-NE-Gel was higher with higher permeation in rat skin.

Conclusion: 5-FU-NE-Gel is found to be for the better to treatment of cutaneous malignancies. It can be developed 5-FU-NE-Gel could be a promising vehicle for the skin cancer chemoprevention.

© 2020 The Author(s). Published by Elsevier B.V. on behalf of King Saud University. This is an open access article under the CC BY-NC-ND license (<http://creativecommons.org/licenses/by-nc-nd/4.0/>).

Abbreviations: 5-FU, 5-Fluorouracil; NE, Nanoemulsion; 5-FU-NE-Gel, 5-Fluorouracil Nanoemulsion Gel; ZP, Zeta Potential; RI, Refractive index; UHPLC-MS/MS, Ultra high performance liquid chromatography mass spectroscopy and mass spectroscopy; Electrospray Ionization, ESI; DDTC, Diethyldithiocarbamate; PDI, Polydispersity Index; SEM, Scanning Electron Microscope; TEM, Transmission Electron Microscope; BCS, Biopharmaceutical Classification System; DSC, Differential Scanning Calorimetry; FT-IR, Fourier-transform infrared spectroscopy; PBS, phosphate buffered solution; ANOVA, Analysis of variance; Kp, Permeability Coefficient; Er, Enhancement Ratio.

* Corresponding author at: Department of Pharmaceutics, College of Clinical Pharmacy, Imam Abdulrahman Bin Faisal University, Dammam, Kingdom of Saudi Arabia-31441 P.O. Box 1982, Dammam 31441, Saudi Arabia.

E-mail addresses: nanhussain@iau.edu.sa, niyazpharma@gmail.com (N. Ahmad).

Peer review under responsibility of King Saud University.



Production and hosting by Elsevier

<https://doi.org/10.1016/j.sjbs.2020.02.014>

1319-562X/© 2020 The Author(s). Published by Elsevier B.V. on behalf of King Saud University.

This is an open access article under the CC BY-NC-ND license (<http://creativecommons.org/licenses/by-nc-nd/4.0/>).

1. Introduction

5-Fluorouracil (5-FU) is used as anticancer medicine in the treatment of many diseases topically like actinic keratosis and non-melanoma skin cancers (Williams, 1971; van Ruth et al., 2006; Tsuji and Sugai, 1983). But the major problem of this drug is lowest optimal delivery due to its poor permeability from the conventional dosage forms like creams and ointments to achieve the therapeutic concentration (Rajinikanth and Chellian, 2016; Saif et al., 2009). There is various skin diseases named as cutaneous premalignant or malignant lesions, psoriasis, and basal cell carcinoma located in the dermis, epidermis, and more deep in the skin layers. It required higher amount of drug delivery in the dermis and epidermis (Kong et al., 2011). Some commercial formulations like Efudex[®], Efudix[®], Carac[®], and Fluoroplex are available for 5-FU topical application as creams or solutions (upto 0.50% 5-FU concentration) to take once-everyday for topical delivery. These commercial preparations have a drawback to a very little retention time when it applied on the site of delivery followed by a low permeation of skin and their retention (Khandavilli and Panchagnula, 2007). These topical commercial preparations have other complications like skin irritation, dryness, redness, burning pain, and swelling. These types of reactions may be extended on for more than two weeks (ElMeshad and Ibrahim, 2011). Though, 5-FU is extremely soluble in water but very poorly permeable containing a very little logP (−0.890). Hence, deep penetration in the skin is very complicated to attain the conventional formulations (Liu et al., 2009).

Topical route is the most common route to deliver the drug directly at the specific site for the treatment of skin cancers locally. Topical route of drug delivery is a non-invasive delivery as compared to parenteral delivery. In addition to via this route we can reduce the systemic toxicities related with the anti-cancerous drugs (Rajinikanth and Chellian, 2016). Marketed 5-FU oral formulations do not exist because of their serious side effects and very low systemic bioavailability. 5-FU showed hydrophilic property; therefore, it is not permeated through dermally or transdermally human stratum corneum which showed the highly lipophilic characteristics. Hence, various efforts have been applied through like microemulsions (Gupta et al., 2005; Elmeshad & Tadros, 2011), transferosomes (Alvi et al., 2011), ethosomes (Zhang et al., 2012), niosomes (Cosco et al., 2009; Alvi et al., 2011), liposomes (Alvi et al., 2011; Thomas et al., 2011), nanoparticles (Zhu et al., 2009; Chauhan et al., 2012), phonophoresis (Meidan et al., 1999), iontophoresis (Fang et al., 2004; Singh & Jayaswal, 2008), electroporation (Fang et al., 2004) and chemical enhancers used (Singh et al., 2005; Khan et al., 2011) have been prepared to enhance 5-FU bioavailability via the transdermal or topical delivery. On the basis of previous reports, microemulsions and nanoemulsions based on oily preparations contains several advantages in comparison to suspensions and emulsions increased solubilization, increased permeation, increased bioavailability with enhanced thermodynamic stability to the delivery of transdermal or topical applications for various lipophilic drugs (Spermath et al., 2007; Elmaghraby, 2008; Hwangl et al., 2009; Ahmad et al., 2019a; Ahmad et al., 2019b; Ahmad et al., 2018a). Hydrophilic drugs via transdermal or topical delivery have not been evaluated through nanocarriers i.e. based on oily preparations (Gupta et al., 2005; Elmeshad & Tadros, 2011).

Hence, the main objective of proposed research is to develop and evaluate a novel w/o nanoemulsions of BCS class III drug i.e. 5-FU using nontoxic, non-ionic with their combination of low HLB surfactant for the treatment of skin cancer through topical delivery. The another aim of this current research have also focused to prepare and compare the effects of the carbopol based

5-Fluorouracil-loaded-nanoemulsion-gel (5-FU-NE-Gel) and 5-FU-NE on melanoma cell lines and the permeation of different skin (i.e. cow, goat, and rats) model studies to determine the penetration and retention of 5-FU concentration. Surgically removed human skin is considered as the “gold standard” for the *ex vivo* penetration study and related with the risk in evaluation of human deep skin layers. But, it is very difficult to collect the human skin on time and also there is a problem in availability with their variations along with samples because of variances in different gender, age, race, and also on anatomical site of the donor (Bronaugh et al. 1982; Bronaugh and Stewart 1985; Sato and Sugibayashi 1991; Panchagnula et al. 1997; Schmook et al. 2001; Vallet et al. 2008; Gupta and Trivedi, 2015). Various models for animal skins from different mammals, reptiles, and rodents have been developed as a substitute for human skin (Gattu and Maibach, 2011.; Vecchia and Bunge 2006). The ethical approval is very essential for the prime research and also restricted. Therefore, we selected cow and goat ear-skin samples for our research study to evaluate the permeation study and it is collected as a waste from slaughter house.

2. Materials and methods

2.1. Materials

5-Fluorouracil was obtained from Chem-Impex International, Inc. Milli-Q-water purification system (ELGA, Made in UK) was used for purification of water i.e. Milli-Q-water. Tween 80, PEG, and other surfactants were bought from Sigma Aldrich. Methanol, ethanol, and acetonitrile (i.e. LC-MS-grade having purity) were bought from Fluka, Sigma Aldrich. Carbopol Smart Polymers was purchased from Bonnymans, solutions for a clean tomorrow, USA (Bar Code: 5159641032).

2.2. Screening of excipients for the preparation of nanoemulsion

The solubility of 5-FU and their stability in nanoemulsion is very important for the use and selection of excipients i.e. co-surfactant, surfactant, and oils. Isopropyl myristate, lauroglycol, Capryol 90, oleic acid, castor oil, arachis oil, and olive oil were chosen as oils. The selection of oils based on easily availability and biodegradability were selected. Tween-20, Span-80, Labrasol[®], Isopropyl Alcohol, Tween-80, Tween-60 and PEG-400 were selected as surfactants. In the vials (5.0 ml capacity) have taken oil (2.0 ml) followed by adding maximum amount of 5-FU and mixed it properly with the help of vortex mixer for the optimization of oil (Ahmad et al., 2019a; Ahmad et al., 2019b). All the samples were centrifuged at 3000.0 rpm for 15.0 min. 5-FU concentration was measured at 266.0 nm in the all above mentioned oils by UV-Spectrophotometer. The selection of surfactant was performed on the basis of addition of selected oil (4.0 ml) mixed with the surfactant solution (2.50 ml, 15.0% v/v surfactant in water) with the help of vortex mixer (Ahmad et al., 2019a; Ahmad et al., 2019b). The mixing was continued awaiting a transparent-clear solution was found. The optimization of co-surfactant was performed in the same way.

Based on highest solubility, pharmaceutical acceptability, non-irritating property, without toxicity, safety and high potential class of constituent, castor oil was selected as the oil phase for preparation of NE. The surfactants were selected on the basis of nonionic property, highest solubility and their safety. The selected surfactants and cosurfactant are Transcutol-HP and PEG-400 respectively. Milli-Q-water was taken as aqueous phase for the preparation of nanoemulsions.

2.3. Pseudo-ternary phase diagrams evaluations and the development of novel nanoemulsions

Different types of nonionic surfactant were selected to prepare the w/o nanoemulsion through the spontaneous emulsification technique. Transcutol-HP (surfactant) and PEG-400 (cosurfactant) were formulated in various weight ratios from one is to zero (1:0) to three is to one (3:1). In the Smix ratio, deionized water was added at a certain point after that oil was added drop by drop until the transparent and clear formulation was found. All diagrams of pseudo-ternary phase were prepared to determine the transparent and clear area (NE-area) (Fig. 1a to 1D) (Ahmad et al., 2019a; Ahmad et al., 2019b). The selections of various formulations is based on solubility of 5-FU in water phase and lowest amount of surfactant and cosurfactant from the every-phase diagrams. 5-FU (1.0% w/w, 10.0 mg/g) was mixed properly in the water and a particular quantity of surfactant and cosurfactant were also added with the help of agitation. Oil is added to develop an oil phase as per the requirement upto the transparent and clear formulation. All these developed formulations were shown in Table 1.

2.4. Thermodynamic stability tests

Various thermodynamic stability evaluations were performed on the newly prepared NEs and the unstable and metastable preparations were also eliminated (Ahmad et al., 2019a; Ahmad et al., 2019b; Ahmad et al., 2018a; Ahmad et al., 2018b). For the evaluation of any phase separation, cracking, creaming, coalescence, all the prepared formulations were centrifuged at 4500 rpm for 30.0 min. On the basis of centrifugation results, we have evaluated the stable formulations and these formulations were again tested for the heating and cooling cycles. We have taken 6-cycles at the temperature between 4.0 °C and 45.0 °C and stored all samples for forty eight hours at every different-temperature. On the basis of heating and cooling cycle's results, all the formulations were selected on their stability and performed again freeze–thaw cycles test for these selected formulation. All the samples were stored at the temperature in-between -21.0 ± 0.50 °C and 20.0 ± 0.50 °C for the 3-cycles for 24.0 h. For more characterization and evaluation, we have taken thermodynamically stable preparations only.

2.5. Newly developed-nanoemulsions characterization

The main parameters were selected i.e. globule size, PDI (polydispersity index), ZP (zeta potential), RI (refractive index), and viscosity for the characterization of newly-developed-NEs. Malvern Zetasizer Nano ZS (Malvern Instruments, Malvern, UK) was used

to characterize NEs in terms of globule size, PDI, and ZP. Scattering angle was examined in between 90.0° at 20.0 ± 1.0 °C for the scattering of the light. In the acrylic-square-cell; each newly-developed-NE has taken near-about 3.0 ml for the measurement of the globule-size and PDI. For the determination of ZP, glass cells were used for the analysis of the samples. Analysis of shape and their texture of optimized-NEs globule, SEM (Zeiss EVO40; Carl Zeiss, Cambridge, UK) and TEM (Morgagni 268D; FEI Company, Hillsboro, OR) were used (Ahmad et al., 2018a; Ahmad et al., 2018b; Ahmad et al., 2018c).

2.6. Preparation of 5-FU-NE-base-gel

Carbopol 934 (1.0 g) was taken for the preparation of 5-FU-NE-base-gel followed by the addition of enough amount of double-distilled-water. When, the dispersion was complete. Carbopol-934 solution was kept to swell totally in the dark at least for 24.0 h. Now, optimized-5-FU-NE was added slowly-slowly in the Carbopol 934 viscous solution with the help of magnetic stirring (Ahmad et al., 2019c). The pH was maintained in-between 6.0 and 9.0 to achieve a homogeneous dispersion gel.

2.7. DSC (Differential scanning calorimetry) analysis

The solubilization and entrapment of the 5-FU in the NE and developed-gel was also evaluated by the DSC 214 Polyma (NETZSCH Wittelsbacherstraße 42, 95,100 Selb, Germany). This analysis was performed on the basis of 5-FU, castor oil, Transcutol HP, PEG-400, optimized-5-FU-NE, Carbopol, and optimized-5-FU-NE-Gel evaluation. An empty pan was used as standard and the sample was taken 10.0 mg in the pan. For the analysis of samples, we have selected the 20.0 °C to 400.0 °C temperature range. This range was based on the 10.0 °K/minutes increase the temperature through the nitrogen flow (60.0 ml/min) (Ahmad et al., 2018a; Ahmad et al., 2019a). For the data-analysis; we used the DSC 214 Polyma (NETZSCH–PROTEUS–70, Germany) software.

2.8. FT-IR study with the help of ATR for the interactions of 5-FU and other excipients

Functional groups of the 5-FU with excipients interaction, chemical structure compounds, and their composition were evaluated by FT-IR based ATR (NICOLET iS50 FT-IR; Thermo Fisher Scientific, 5225 Verona Road, Madison, WI 53711, USA). The IR–spectra of pure 5-FU, castor oil, PEG-400, Transcutol HP, 5-FU-NE, and 5-FU-NE-Gel were examined through an attenuated total reflectance ($4000\text{--}400\text{ cm}^{-1}$ wavenumber range of ATR). Pure 5-FU, castor oil,

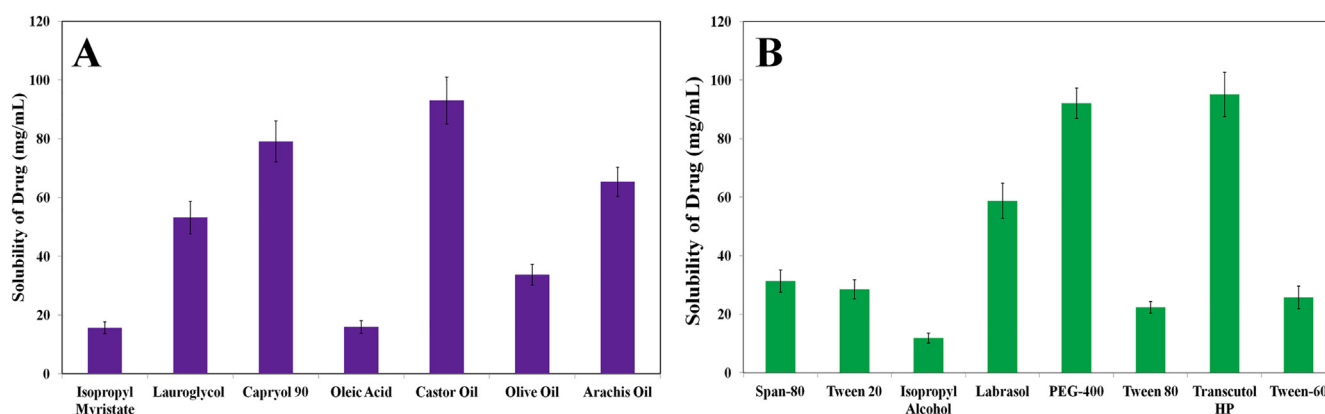


Fig. 1. Solubility of 5-FU determined in different types of oils and surfactants.

Table 1

Formulation components of nanoemulsions of 5-FU (FU-NE1–FU-NE9) prepared using Castor Oil (Oil Phase), PEG-400(co-surfactant), Transcutol-HP (Surfactant) and deionized water (Aqueous Phase).

Composition of Formulation (% w/w)					
Code for Formulation	Castor Oil	Transcutol-HP	PEG-400	Water	S _{mix} ratio
FU-NE1	50	20	20	10	1 : 1
FU-NE2	45	20	20	15	1 : 1
FU-NE3	40	27	13	20	1 : 1
FU-NE4	50	27	13	10	2 : 1
FU-NE5	45	27	13	15	2 : 1
FU-NE6	30	34	16	20	2 : 1
FU-NE7	50	29	11	10	3 : 1
FU-NE8	45	29	11	15	3 : 1
FU-NE9	30	37	13	20	3 : 1

PEG-400, Transcutol HP, 5-FU-NE, and 5-FU-NE-Gel were directly analyzed without any special preparation.

2.9. Release study of 5-FU (In vitro)

Release study of 5-FU from optimized-NE was carried out by the dialysis membrane (treated before) (pore size: 2.4 nm–molecular-weight cut-off ~12–14 kD) (Sood et al., 2014; Ahmad et al., 2018a; Ahmad et al., 2018b; Ahmad et al., 2018c). First we prepared the release medium (phosphate buffer; pH: 7.4 = 1.0 L). The temperature was maintained at 37.0 ± 1.0 °C with the help of stirrer upto 6 h at 1 rcf. Finally, the dialysis bag was properly checked for any leakage and it was placed inside 5-FU-NE (containing 0.50 mg 5-FU). For the 5-FU-release study from the 5-FU-NE selected predetermines selected time points (i.e. 30, 60, 120, 240, 360, 480, 720, 1440 min). At every time point, we have withdrawn the test samples (1.00 ml). All these test samples were filtered first by syringe filter (0.450 µm) first after that 5-FU quantity was analysed by the in-house developed-UHPLC-MS/MS-method.

2.10. Refractive index (RI) and viscosity

Viscosity and RI tests were carried out on the basis of Ahmad et al. method (Ahmad et al., 2018a; Ahmad et al., 2018b; Ahmad et al., 2018c).

2.11. Stability studies for 5-FU-NE3

Physical stability studies were performed for the selected FU-NE3 on the basis of transdermal permeation data and physico-chemical characterization. In this test, FU-NE3 test samples were kept at 4.0 °C (refrigerator temperature). Different types of physico-chemical parameters i.e. RI, viscosity, ZP, PDI, and droplet size were evaluated at 0, 30, 60, and 90 days. In this way NE-characterization were performed.

2.12. 5-FU permeation evaluation on different skin

Ear pinna Skin from Goat and cow were taken and also swiss albino rat full thickness skins (CGR Skin) have been used for the permeation studies. All the skins were cleaned with cold water followed by the removal of non-dermatome skin by the scalpel. Optimized-nanoformulations i.e. FU-NE3, 5-FU-NE3-Gel and 5-FU-saturated aqueous solution was performed on a Franz diffusion cells (0.785 cm² diffusional area) and receiver chamber (~12.0 ml capacity) for the *ex vivo* permeation on different animal's skin (cow, goat, and rat: CGR). *Ex vivo* permeation studies were performed on the automated Logan transdermal diffusion cell sampling system (DHC-6T, Logan Instrument Corporation, Avalon, NJ). Researchers have taken the IRB approval from the IRB ethical committee of Imam Abdulrahman Bin Faisal University to conduct this research study with ethical approval number IRB-UGS-2019-

05-379. Phosphate buffer saline (PBS, 12.0 ml, 7.4-pH) filled in the receptor compartment followed by the stirred with a magnetic bar. The receptor compartment was maintained a constant temperature (37.0 ± 1.0 °C). DHC-6T instrument was washed and stabilized for 10.0 min. After stabilization, 1.0 g of FU-NE3 and 5-FU-NE3-Gel nanoformulation (10.0 mg g⁻¹ 5-FU) or 1.0 g of saturated aqueous solution (10.0 mg/g) was kept into every donor compartment. 5-FU saturated aqueous-solution was taken as control to determine the enhancement factor (Ef). All the withdrawn samples were evaluated at sampling time points (1, 2, 4, 6, 8, 10, 12.0, and 24.0 h) by the automated sampler in the UHPLC-MS/MS vials and then again filtered through a 0.25 µm syringe filter into the fresh UHPLC vials. Analysis of all the samples were performed for the 5-FU permeated concentration through the in house developed and validated UHPLC-MS/MS-method.

2.13. Retention or deposition of 5-FU studies on the different animal's skin

Finally the permeation study was completed the surplus amount of formulation was washed properly and SC was cleaned through the striping with adhesive tape. The quantity of 5-FU was determined by cutting small pieces of remaining skin in the viable skin parts i.e. epidermis and dermis. Skin viable part and Tape strips were pooled in the phosphate buffer solution having pH = 7.40. For the evaluation of 5-FU from the extract, we have vortexed and sonicated the extract followed by centrifugation process.

For the quantification of the 5-FU, a UHPLC-MS/MS method was used. In the eppendorf tube, the sample was taken (90 µL) which was mixed properly with sodium DDTC solution (10.0 ml, 10% w/v) which was prepared in sodium hydroxide (0.1 N). We maintained the 37.0 °C temperature with the help of water bath upto 1.0 h for incubation of samples. All the samples were cooled with the help of ice-bath for the completing the processes i.e. 5-FU-DDTC chelates formation.

These chelates were extracted with 100.0 ml of chloroform by vortexing at maximal speed for 1 min and centrifuged at 5000 rpm for 5 min at 5 °C. The extraction of 5-FU-DDTC chelates was performed in the chloroform (100.0 ml) which was vortexed with high speed upto 1.0 min followed by centrifugation (5000 rpm) at 5.0 °C for 5.0 min. After that, 10.0 ml of the chloroform layer was taken and dried in Nitrogen evaporator. These mixtures were reconstituted with 750 µL mobile phase (Methanol: 5 mM Ammonium Formate::75:25) followed by vortexing. These reconstituted samples has been transferred into UHPLC-vials and injected to UHPLC-MS/MS analysis.

2.14. UHPLC-MS/MS analysis of 5-FU

To develop a method, UHPLC-MS/MS i.e. Pinnacle DB C18 (1.9 µm; 50 × 30.0 mm) using a binary solvent manager autosampler with very sensitive and high resolution tunable mass detector

(LCMS-8050, ESI, Triple Quadrupole, Japan), was used. Chromatographic conditions was used as a Pinnacle DB C18 (1.9 μm ; 50 \times 30.0 mm) were as; mobile phase (Methanol: 5 mM Ammonium Formate::75:25), flow rate (0.150 ml/min) and injection volume (10.0 μL). DDTC and DDTC–Platinum complex were eluted at 0.736 and 2.185 min respectively (Fig. 9).

2.15. Analysis of permeation studies on various animals' skins

Permeation of 5-FU was determined by the various animal's skin (cow, goat, and rat; $\mu\text{g}/\text{cm}^2$) for every 5-FU-NE, 5-FU-NE-gel nanoformulation with control (5-FU-S). Steady state (J_{ss}) for all types of skin, was calculated by permeability coefficient (K_p) multiplied with initial concentration of 5-FU (C_0) in the donor compartment. The graph was plotted in-between cumulative 5-FU permeation ($\mu\text{g}/\text{cm}^2$) with time (hours) through predetermined diffusion cell area. Er (enhancement ratio) and K_p (permeability coefficient) were determined by the use of Eqs. (2) and (1), respectively (Shakeel et al., 2009):

$$K_p = \frac{J_{ss}}{C_0} \quad (1)$$

$$Er = \frac{J_{ss} \text{ of formulation}}{J_{ss} \text{ of control}} \quad (2)$$

2.16. Various types of skins interaction studies

Various types of skins (cow, goat, and rats) sections were used to evaluate the interactions due to the 5-FU permeation were estimated under the fluorescence microscope. 6-carboxyfluorescein i.e. a water soluble fluorescence probe was taken for different types of nanoformulations. All the animal's skin were washed with phosphate buffer solution (pH 7.40) which were kept in different Franz diffusion cells and treated with separate prepared and optimized nanoformulations after the incubation i.e. 10.0 h (37.0 \pm 1.0 $^\circ\text{C}$). Different skin sections were cut with the help of cryostat microtome (25.0 mm thickness) followed by mounted with 6-carboxyfluorescein solution glass microscope slide and observed under the fluorescence microscope (ProgRes CP-SCAN, LASER OPTIC SYSTEM, USA).

2.17. Melanoma cell lines used for cytotoxicity studies

Melanoma cell lines (SK-MEL-5, malignant) were used for *in vitro* cytotoxicity with their comparative effects of optimized-5-FU-NE3 and 5-FU-NE3-Gel with its aqueous solution and control. Optimized-NE3-Gel (i.e. Placebo without the drug: 5-FU) was used as control. WST-1 [2-(4-iodophenyl)-3-(4-nitrophenyl)-5-(2,4-disulphophenyl)-2H-tetrazolium] assay was employed as to examine cytotoxic effects. RPMI-1640 cultured medium were used for the SK-MEL melanoma cells, fetal bovine serum (10.0% FBS), ABM (1.0% GIBCO), penicillin (100 IU/mL), streptomycin (100 mg/mL) and L-glutamine (2.0 mmol^{-1}) at 37.0 $^\circ\text{C}$ in the atmosphere of 5% CO_2 . Various concentrations of 5-FU-S, NE3-Gel i.e. control, optimized-5-FU-NE3, and 5-FU-NE3-Gel were taken to replace with fresh medium in the same amount of volumes. WST-1 reagent (10.0 ml) was taken after 72.0 h for the re-incubation (for 4.0 h) of each and every plate at 37.0 $^\circ\text{C}$. ELISA reader was used to determine the quantity of formazan at 450.0 nm.

2.18. Statistical evaluation

The entire results were evaluated as mean \pm SD ($n = 3$). Characterization and optimization, skin permeation, and cytotoxicity

studies were examined with statistics through the analysis of variance (ANOVA) using Student's *t* test to examine the significant differences.

3. Results and discussion

3.1. Screening of excipients

Based on reported literature, the solubility of water-soluble/hydrophilic drugs in the oil is also very important for the screening of excipients (Ahmad et al., 2018d; Ammar et al., 2009). The proposed medicine i.e. 5-FU is water-soluble i.e. hydrophilic in nature. In the proposed plan w/o nanoemulsion, the internal phase is aqueous phase and it should be solubilized because it will come in contact to medium i.e. easily soluble in the water based media (Singh et al., 2005). Oil soluble-drugs i.e. lipophilic in nature, it is better to plan formulate the o/w nanoemulsion. On the other side, w/o system appears to be a very good selection for hydrophilic drugs. For the delivery of therapeutic dose, the amount of formulation must be reduced as much as possible. For the oil phase, the 5-FU solubility was very essential parameter in the oils. For the solubilization of 5-FU, surfactant and co-surfactant are also very important. For the development of nanoemulsions, 5-FU solubility was examined in the different types of oils, co-surfactants and surfactants are indicated in Fig. 1. Castor oil has been selected as oil-phase for the preparation of nanoemulsion due to the highest solubility in comparison other oils. 5-FU is soluble in water because of this to formulate the w/o nanoemulsion. The most important parameter is based on drug delivery related to the toxicity of the surfactants for the preparation of nanoemulsion. Huge quantity of surfactants may produce irritation to the skin via transdermally delivery. For the transdermally delivery, it is very important to examine the concentration of surfactants that should be use low amount at time of formulation of nanoemulsion. It is previously reported that Non ionic surfactants are more safe as compared to ionic surfactants (Pouton and Porter, 2008; Shakeel and Ramadan, 2010). Zwitterionic or Non-ionic surfactants are considered as highly safe in the pharmaceutical therapeutic purposes at the time of formulation development of nanoemulsions and also less influenced through pH anionic strength changes followed by doesn't cause any irritation to the skin. Generally, it is very difficult to obtain the required interfacial area in the use of only one surfactant. Although the use of co-surfactant at the time of development of formulation, it showed the additive effects of both surfactants. It will not adversely affect the absorption of drug to each-other. It is also observed that mixed micelle preparations do not decrease the present quantity of surfactant molecule concentration. The cosurfactant also knows as second amphiphile. We have selected the surfactant (Transcutol HP) and co-surfactant (PEG-400) on the basis of maximum solubility of 5-FU containing the nature of non-ionic property and non-toxicity (Fig. 1) (Shakeel and Ramadan, 2010; Kotta et al., 2015; Narkhede et al., 2014). Another most important benefit is also here for the selection of Transcutol HP as a surfactant contained a very low HLB-value which will be more beneficial for the development of the w/o stable nanoemulsion development. Here, aqueous phase was taken as deionized water and it is more required as aqueous medium for the preparation of nanoemulsion (Shakeel and Ramadan, 2010).

3.2. Pseudoternary phase diagrams preparation and their tests for thermodynamic stability

The best optimized-nanoemulsion was characterized by their relationship between the phase behavior and all the components can be determined by pseudo-ternary phase diagram (Lawrence

and Rees, 2000). For each Smix ratio, pseudo-ternary phase diagrams were built separately in order that accurate regions of nanoemulsion (w/o) could be recognized (Fig. 2). Various nanoemulsions were formulated on the basis of pseudo-ternary phase diagrams (Fig. 2A to 2D) with the results of various thermodynamic stability tests. 5-FU (10.0 mg, 1.0% w/w) was dissolved in the water. Surfactant and cosurfactant (S_{mix}) was mixed as per the required quantity in many ratios (3:1, 2:1, and 1:1) with added drop by drop in the oil phase until a clear and transparent formulation was found (Table 1). Smix ratio (3:1) has shown lowest nanoemulsion area in the Fig. 1D. Highest solubility of oil was found in S_{mix} ratio (1:1) from the phase diagram (Fig. 1B). We added the cosurfactant with surfactant then area of nanoemulsion enhanced very fast. The nanoemulsion region for Smix ratio (2:1, in the Fig. 1C) was little bit increased but not more. The nanoemulsion area for Smix ratio of 1:0 (Fig. 1A) was reduced slightly in comparison of 1:1.

For the removal of unstable and metastable formulations, all the prepared-NEs were tested for various thermodynamic stability parameters (Shakeel and Ramadan, 2010; Ahmad et al., 2018a; Ahmad et al., 2018b; Ahmad et al., 2018c). All the developed formulations tested for creaming, any phase separation, coalescence or cracking by the centrifugation at 4500.0 rpm for 30.0 min. The

developed formulations passed the stability test by the centrifugation processes followed by the heating and cooling cycles. Refrigeration of 6-cycles at the selected temperature (4.0 °C) & 45.0 °C for 2-days were tested. The stability test passed formulations from heating and cooling cycle's tests that were chosen for freeze thaw cycles. For each temperature -21.0 °C and 20.0 °C, the 3-freeze-thaw-cycles were performed for 24.0 h. Thermodynamically stability test passed nanoformulations were taken for more characterization and their evaluation.

3.3. 5-FU-NEs characterization

All the physicochemical examination results for 5-FU-NE (FU-NE1 to FU-NE9) are shown in Table 2. Thermodynamically stability test passed-formulations were more characterized by the globule-size, PDI, zeta potential, RI, and the viscosity. The optimized-5-FU-loaded-NE is further characterized by globule size i.e. very important. 5-FU-NE (FU-NE1 to FU-NE9) globule sizes were measured i.e. 66.97 ± 2.46 to 206.45 ± 7.98 nm as presented in Table 2. FU-NE7 was showed largest globule-size it may be due to the maximum concentrations of oil i.e. 50% w/w followed by also higher surfactants concentration i.e. Smix (40.0% w/w) as presented in the Table 2. FU-NE1 to FU-NE9 nanoemulsions showed the droplet size

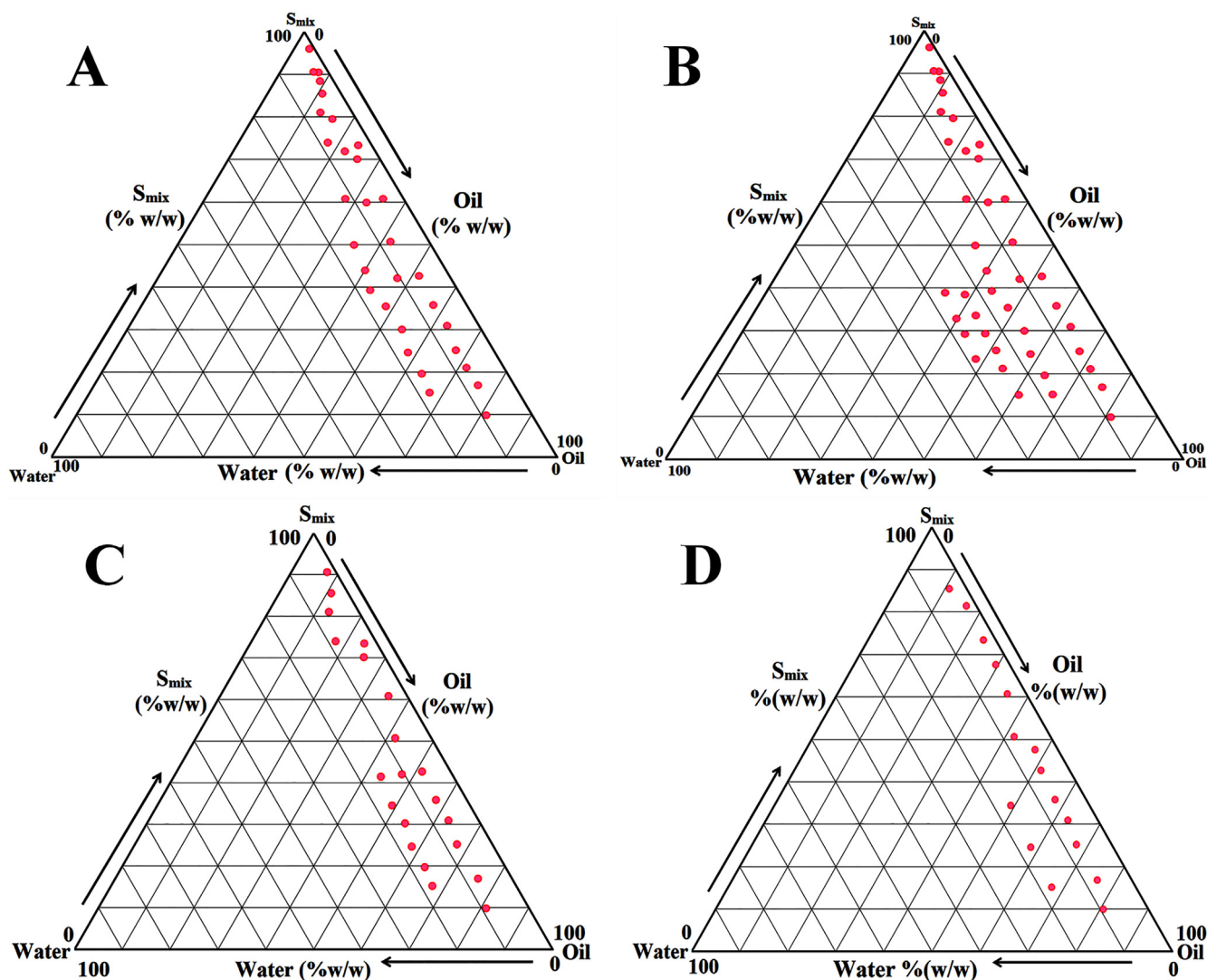


Fig. 2. Zones of Nanoemulsions (w/o) evaluated by pseudo-ternary phase diagrams in which deionized water is used as aqueous phase, castor oil (oil phase), Transcutol-HP (surfactant), and PEG-400 (cosurfactant) on the various concentrations of Smix ratios [1:0 (A), 1:1 (B), 2:1 (C) and 3:1 (D)].

increased with increased in the oil concentration. FU-NE3 nanoformulation was showed the smallest globule size (66.97 ± 2.46 nm) that can be small quantity of oil concentration with optimum Smix surfactants concentration. FU-NE1 to FU-NE9 nanoformulations globule size enhanced with enhanced the surfactants and Smix ratio concentration. The uniformity of globules is also related with PDI of nanoformulation. The uniformity of globules is high with smaller the PDI value within the formulation. All the formulations showed the < 0.452 PDI, it showed the uniformity of globule sizes within the formulations. FU-NE3 nanoformulation showed the smallest PDI value i.e. 0.216 ± 0.020 that means maximum uniformity of droplet sizes (Table 2).

Zeta potential values of nanoemulsions FU-NE1 to FU-NE9 were found in the range of -29.65 to -21.63 mV. If the ZP values showing the range of ± 25.0 to -30.0 mV described as a stable nanoformulation (Craig et al., 1995; Ahmad et al., 2019a). 5-FU-Nanoemulsions (FU-NE1 to FU-NE9) determined the higher enhancement in the globule size as comparison to PDI that also displayed very less differences and higher uniformity of the distribution in globule size along with all the prepared formulations (Ahmad et al., 2019a). Total surface charge and their stability of the optimized-5-FU-NE is also determined by the zeta potential i.e. also very important. In the Table 2, zeta potential values of optimized nanoformulations (FU-NE1 to FU-NE9) were determined -29.65 to -21.63 mV. The lowest zeta potential value was found in the 5-FU-NE7 i.e. -29.65 mV. The maximum zeta potential value was observed in the 5-FU-NE7 i.e. -21.63 mV. There was also significant alteration seen in ZP values in-between from FU-NE1 to FU-NE3, FU-NE4 to FU-NE6, and FU-NE7 to FU-NE9 nanoemulsions ($p < 0.050$). The developed-NEs were exhibited stability as physically & thermodynamically. If the ZP has showed negative values may be because of fatty acids and esters in the castor oil (Ahmad et al., 2019a). FU-NE1 to FU-NE9 optimized-nanoemulsions was observed the RI-range i.e. 1.362 ± 0.012 to 1.830 ± 0.031 (Table 2). All the RI including FU-NE1 values were found very near to RI of castor oil (RI: 1.47–1.48) as external oil phase used to the formulation of NEs. All the mentioned RI-values are for the characterization of nature nanoemulsions like w/o of 5-FU-loaded-NEs. Dynamic light scattering (DLS) do not depend on the ZP for light scattering but it depends on the RIs followed by globule-size. In the Table 2 showed the data for the RIs i.e., 1.362 ± 0.012 to 1.830 ± 0.031 FU-NE1 to FU-NE9 and it designates not so much variations. RIs have not affected by light scattering and exhibited RIs very close to water (1.441) for FU-NE3. Thus, it is a sign of the transparent nature and water-in-oil (w/o) of FU-NE3 type behavior (Bhattacharjee, 2016). The viscosity of developed nanoemulsions (FU-NE1 to FU-NE9) was observed in the range of 52.31 ± 2.98 to 123.47 ± 6.69 cps (Table 2). FU-NE3 viscosity was observed smallest 52.31 ± 2.98 cps in comparison of all formulations. It may be due to smaller castor oil concentration (Ahmad et al., 2019a; Ahmad et al., 2019b).

If the quantity of the Smix has been increased, it showed that the viscosity of 5-FU-NE3 altered radically. So, the concentration of castor oil decreased from FU-NE1 to FU-NE3, FU-NE3 to FU-NE6, and FU-NE7 to FU-NE9 as same as according to the viscosity decreased radically (Table 2). Furthermore, all FU-NE1 to FU-NE3, FU-NE3 to FU-NE6, and FU-NE7 to FU-NE9 as same as according to viscosity decreased with the reduction of oil concentration followed by same reduction in globule size of the prepared formulations (Table 2). So these parameters are very important to affect the viscosity of the 5-FU-NE by Smix and oil concentration. Alternatively, lower concentration of castor oil (40%) with the small globule size and water (20%) showed a very good effect on 5-FU-NE3 viscosity. At last, the minimum and highest viscosities were identified in the FU-NE3 (52.31 ± 2.98 cp) and FU-NE7 (123.47 ± 6.69 cp), respectively. The smaller value of viscosity is responsible for the free flowing behavior of all 5-FU-NEs (FU-NE1 to FU-NE9).

Determination of transmission (%) is very important to evaluate the clear behavior of the optimized-5-FU-NEs. All developed 5-FU-NEs (FU-NE1 to FU-NE9) showed the 92.67 ± 0.16 – 99.54 ± 0.04 % transmission in the Table 2. 5-FU-NE (FU-NE3) showed the highest %transmission (99.54 ± 0.04 %) on the other side 5-FU-NE (FU-NE7) indicated the lowest value of %age transmission i.e. 92.67 ± 0.16 %. All 5-FU-NEs indicated transparent nature of all nanoformulations. Finally, we have chosen 5-FU-NE (FU-NE3) on the basis of optimized globule-size, PDI, optimum-required-ZP, smallest viscosity and RI due to highest stable nanoformulation as reported before (Ahmad et al. 2019a; Ahmad et al., 2019c; Ahmad et al. 2018a; Ahmad et al. 2018b; Ahmad et al. 2018c; Ahmad et al. 2018d) and containing a greatest %age transmittance. Optimized 5-FU-NE (FU-NE3) was found -21.63 mV zeta potential (Fig. 3B). Oil globules agreed to a total amount of globule charge is due to the stability of nonionic surfactants (Ahmad et al. 2019a). Shape and their surface texture of 5-FU-NE were examined by SEM and TEM. 5-FU-NE (FU-NE3) showed the smooth and round surface analysed by SEM (Fig. 3C). The morphological behavior of Optimized-5-FU-NE (FU-NE3) was determined by TEM analysis. The surface morphology of globule and their size were determined by TEM analysis (Fig. 3D). 5-FU-NE3 exhibited all globule sizes in the range of nanometer by the TEM analysis (Fig. 3D). The globules sizes of 5-FU-NE3 exhibited spherical shape because of castor oil and Transcutol HP (Ahmad et al., 2019a). Therefore, on the basis of above characterization and results observation, our nanoemulsion (FU-NE3) fits to the further research studies.

3.4. DSC analysis

As per the COA, 5-FU showed in-between the range 282 – 283 °C melting point peak. An endothermic peak identified 282.50 °C for 5-FU by the DSC analysis (Fig. 4) and confirmed the crystalline nature of 5-FU. DSC of castor oil (a single line), Transcutol HP exhibited various peaks like 45.9 °C, 167.9 °C, 172.6 °C, 213.0 °C, and

Table 2
Characterization of developed-Nanoemulsions.

Code for Formulation	Globule Size (nm)	PDI	Zeta Potential (mV)	RI \pm SD	Viscosity \pm SD (cps)	% Transmittance
FU-NE1	121.39 ± 5.06	0.398 ± 0.029	-28.36	1.601 ± 0.013	109.57 ± 6.32	96.64 ± 0.07
FU-NE2	95.84 ± 3.67	0.318 ± 0.027	-26.48	1.493 ± 0.034	93.48 ± 4.03	97.64 ± 0.06
FU-NE3	66.97 ± 2.46	0.216 ± 0.020	-21.63	1.362 ± 0.012	52.31 ± 2.98	99.54 ± 0.04
FU-NE4	183.83 ± 7.62	0.416 ± 0.036	-29.01	1.789 ± 0.026	119.63 ± 6.19	94.26 ± 0.09
FU-NE5	151.70 ± 4.07	0.391 ± 0.026	-28.10	1.534 ± 0.027	110.03 ± 5.32	95.67 ± 0.08
FU-NE6	139.66 ± 3.83	0.373 ± 0.020	-25.79	1.498 ± 0.024	97.75 ± 4.87	94.54 ± 0.10
FU-NE7	206.45 ± 7.98	0.452 ± 0.041	-29.65	1.830 ± 0.031	123.47 ± 6.69	92.67 ± 0.16
FU-NE8	176.56 ± 5.67	0.401 ± 0.032	-28.72	1.593 ± 0.030	112.81 ± 5.58	93.94 ± 0.17
FU-NE9	159.02 ± 4.31	0.351 ± 0.026	-27.13	1.451 ± 0.021	99.34 ± 4.69	95.84 ± 0.11

PDI: Polydispersity Index, nm: nanometer, RI: Refractive Index, SD: Standard Deviation, mV: milli volt, cps: cycles per second.

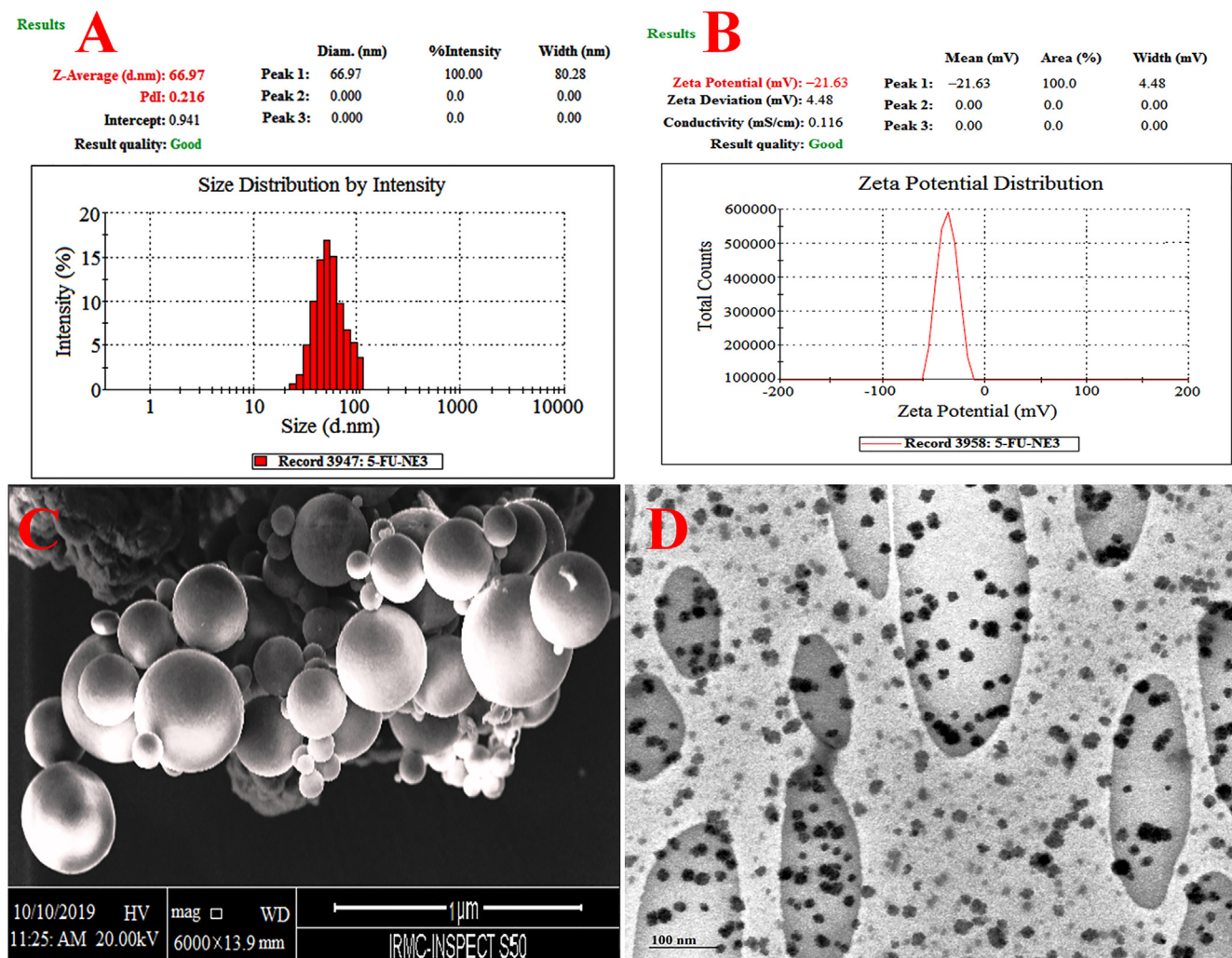


Fig. 3. Distribution of 5-FU-NE is determined by dynamic light scattering techniques (A), zeta potential of 5-FU-NE (B), SEM images (C), and TEM images (D).

PEG-400 (36.8 °C, 263.7 °C, and 270.3 °C). Optimized-5-FU-NE (FU-NE3) has given three peaks for Transcutol HP and PEG-400 in the DSC thermogram. There was no peak for 5-FU in the Optimized-5-FU-NE (FU-NE3) DSC thermogram. Finally, it was concluded that 5-FU entirely entrapped inside the core of nanoemulsion. Carbopol showed the three major peaks (63.3 °C, 115.2 °C, and 146.9 °C). Finally, optimized-5-FU-NE-Gel showed various very small peaks for other ingredients like Transcutol HP, PEG-400, carbopol in the thermogram of DSC except 5-FU (Ahmad et al., 2018b; Ahmad et al., 2019a).

3.5. 5-FU-excipients interactions evaluation ATR-based FT-IR

Pure 5-FU, castor oil, PEG-400, Transcutol HP, 5-FU-NE, and 5-FU-NE-Gel were evaluated through FT-IR as shown in the Fig. 5. Pure 5-FU, castor oil, PEG-400, Transcutol HP, 5-FU-NE, and 5-FU-NE-Gel were analysed by the ATR-based FT-IR spectroscopy. The surfaces of NE were evaluated through the ATR spectroscopy which can be used for both purposes qualitatively and quantitatively (Wan et al. 2018; Ahmad et al. 2018c; 2019c). 5-FU exhibited their characteristic stretching band of -NH at 3119.14 cm^{-1} ; other symmetric aromatic ring stretching at 1720.17 cm^{-1} (C=O), 1640.30 cm^{-1} (C-N), 1242.73 cm^{-1} (C-F), and 1180 cm^{-1} (C-O) peak was showed. Transcutol HP was obtained the characteristics peaks at 3427.92, 2865.10, 1827.84, 1746.84, 1698.08, 1456.90,

1351.08, 1268.91, 1105.37, 1064.34, 940.17, 886.09, 838.65, 764.47, 650.14, and 564.52 cm^{-1} . PEG-400 was found the characteristics peaks at 3450.23 (O-H), 2864.55 (C-H), 1458.11 (C-H bending), 1352.73 (C-H bending), 1290.13 & 1093.84 (O-H & C-O-H stretching), 942.20, 838.92, 764.31, 650.45, and 565.66 cm^{-1} . Castor oil was obtained the characteristics peaks at 3412.85 cm^{-1} (-OH stretching); 2924.23 cm^{-1} (-CH₂ asymmetric stretching); 2853.96 cm^{-1} (-CH₂ symmetric stretching); 1741.77 cm^{-1} (-C=O); 1152.85 cm^{-1} (C-O-C). In the spectrum of 5-FU-NE, strong absorption bands at 3400.35, 2924.14, 2854.54, 1741.78, 1458.33, 1349.02, and 1099.15 cm^{-1} were clearly showed and it means the entrapment of 5-FU-NE in the nanoemulsion. Transcutol HP showed a peak due to the presence of OH-stretching with higher intensity for this peak as compared to 5-FU peak was partially recognized to the H₂-bonding between 5-FU and Transcutol HP. 5-FU-NE attained all the distinctive peaks of NE. However, 5-FU-distinctive peak in the 5-FU-NE was not identified. ATR-FTIR spectroscopy was used to investigate the surface of NE. 5-FU-NE showed 5-FU entrapped inside the 5-FU. The amount of 5-FU is inconsequential to detect as compared to 5-FU-NE while a little quantity of 5-FU can be there on the surface of NE. At the end, it means there was no chemical reaction between 5-FU and other ingredients of the optimized-nanoformulation (Wan et al. 2018; Ahmad et al. 2019a; Gupta and Trivedi, 2015). Now it is cleared that most of the amount of 5-FU is entrapped

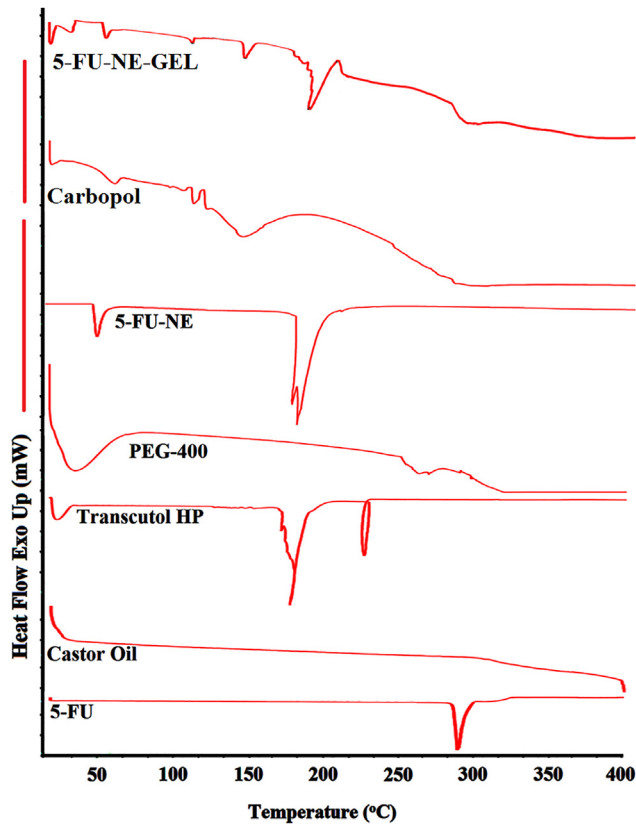


Fig. 4. DSC-thermograms showed endothermic peaks of castor oil, 5-FU, Transcutol HP, PEG-400, 5-FU-NE, Carbopol and freeze dried optimized-5-FU-NE-Gel.

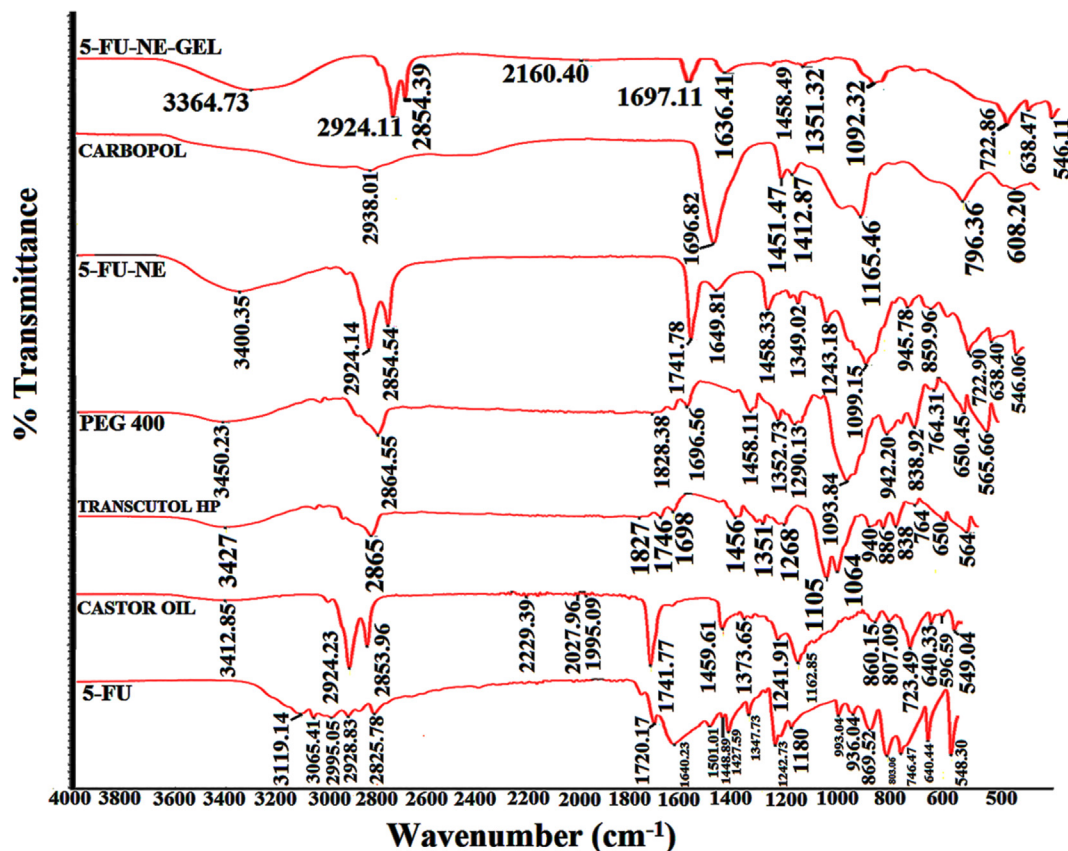


Fig. 5. Spectral analysis of ATR of castor oil, 5-FU, Transcutol HP, PEG-400, 5-FU-NE, Carbopol and freeze dried optimized-5-FU-NE-Gel.

inside the core of the NE. We didn't find any types of isomerization product i.e. to stimulate the stability and biological activities of 5-FU. The Carbopol spectra exhibited one OH-stretching peak at the 2938.01 cm^{-1} , a prominent C=O peak at 1696.82 cm^{-1} and peaks at 1451.47 & 1412.87 cm^{-1} which indicated for the C–O and O–H functional groups. At last, COO of carboxylic acid in acrylate spectra showed a peak for carbopol 940 at 1636.41 cm^{-1} in 5-FU-NE-Gel nanoformulation (Fig. 5).

3.6. *In vitro* 5-FU release studies

The initial release of 5-FU-S 78.16% at 30.0 min and the end 100% released at 2.0 h (Fig. 6). 5-FU released $15.48 \pm 2.88\%$ and $30.55 \pm 2.97\%$ in 1.0 h which was an initial burst release from optimized-5-FU-NE and optimized-5-FU-NE-Gel after that maintained a sustained release in Fig. 6. At the end, 5-FU was released from optimized-5-FU-NE and optimized-5-FU-NE-Gel i.e. 65.48% and 80.13%. 5-FU burst was released initially from optimized-5-FU-NE and optimized-5-FU-NE-Gel due to the 5-FU eroded outer layer from the 5-FU-NE and 5-FU-NE-Gel. Finally, 5-FU-NE entrapped inside the core of the nanoemulsion and same is in gel nanoformulation (Ahmad et al. 2019c; Ahmad et al., 2019d). For optimized-5-FU-NE-Gel, 5-FU released to fit in the various kinetics models that contain highest value for R^2 was fit to the many high standard release model (*in vitro*) for 5-FU from 5-FU-NE-gel. The highest value fitted to Higuchi model i.e. $R^2 = 0.9794$. The value of correlation coefficient (R^2) was find out i.e. 0.9693 and after that zero order ($R^2 = 0.9451$) followed by Korsmeyer–Peppas. The most important parameter i.e. initial burst release of 5-FU was observed a sustained release that is useful to achieve the highest concentration gradient participated in the successful transdermal delivery of 5-FU (Ahmad et al. 2019c; Ahmad et al., 2019d).

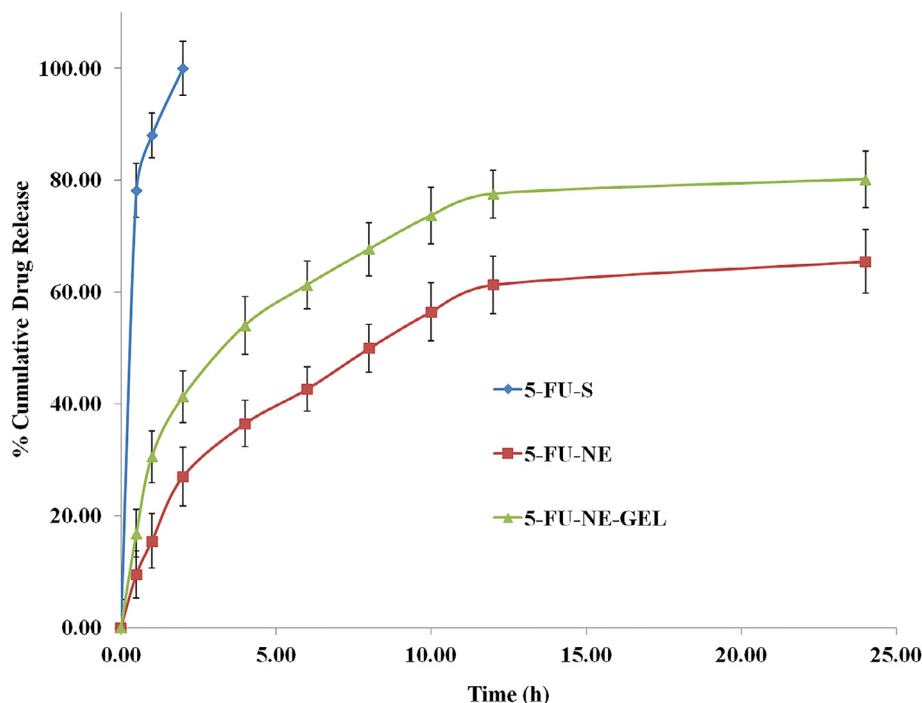


Fig. 6. showed the %age-cumulative-release of 5-FU from 5-FU-NE and 5-FU-NE-Gel when it compared with pure 5-FU-S.

3.7. 5-FU permeation, retention and evaluations of their data by ex vivo

5-FU permeated through the cow, goat skin from ear pinna, and swiss albino rat skin (CGR Skins) different types of formulations ex vivo in the Fig. 7. 5-FU-NE-Gel showed the excellent delayed 5-FU permeation via the CGR skins. The permeation of 5-FU from 5-FU-NE-Gel nanoformulation for rat skin model was 1.25 times greater than the cow and goat skin model. The permeation of 5-FU from 5-FU-NE-Gel nanoformulation for rat skin model was 1.56 times higher than the 5-FU-NE and 12.51 times higher than the 5-FU-S for the cow and goat skin model. The permeation of 5-FU have not found significant difference between cow and goat skin model ($p > 0.5$). However, there was evaluated a statistically significant in-between rat versus cow i.e. $p < 0.01$ on the other side also found that rat versus goat skin model ($p < 0.01$) for the permeation of 5-FU from 5-FU-NE-Gel. Permeability coefficient (K_p), steady-state flux (J_{ss}), and Enhancement Ratio calculated as represented in Table 3. For the evaluation of mentioned parameters, 5-FU-S was selected as reference/control. Permeability coefficient

and steady-state flux were significant in final opt-NE with their opt-NE-Gel followed by 5-FU-NE3 and 5-FU-NE3-Gel as compared to 5-FU-S ($p < 0.01$ and $p < 0.001$). Er showed to be maximum (8.58; 5-FU-NE3 and 10.34; 5-FU-NE-Gel) for goat skin compared with other optimized-nanoformulations. J_{ss} and K_p values for 5-FU-NE3 and 5-FU-NE3-Gel were found to be highest for rat skin i.e. 10.345 ± 0.97 (5-FU-NE3); 12.0244 ± 1.12 (5-FU-NE3-Gel) $\mu\text{g}/\text{cm}^2/\text{h}$ and 1.0345 ± 0.061 (5-FU-NE3); 1.2024 ± 0.073 (5-FU-NE3-Gel) $\mu\text{g} \times 10^{-3}$, respectively (Table 3). J_{ss} and K_p values for 5-FU-NE3-Gel were determined to be $12.0244 \pm 1.12 \mu\text{g}/\text{cm}^2/\text{h}$ and $1.2024 \pm 0.073 \mu\text{g} \times 10^{-3}$, respectively, which were also highly significant in comparison of 5-FU-S ($P < 0.001$). The same results were also found with cow and goat skin when it compared to 5-FU-S in terms of the values of J_{ss} and K_p i.e. highly significant. 5-FU-NE3 and 5-FU-NE3-Gel increased permeability parameters due to smallest viscosity, smallest droplet size, and optimum concentrations of castor oil, Transcutol-HP, and PEG-400. All the data related with 5-FU % permeation, accumulation into the SC and viable skin represented in Fig. 11. 5-FU concentration of permeation and partitioning showed into various compartment of the skins i.e. SC and

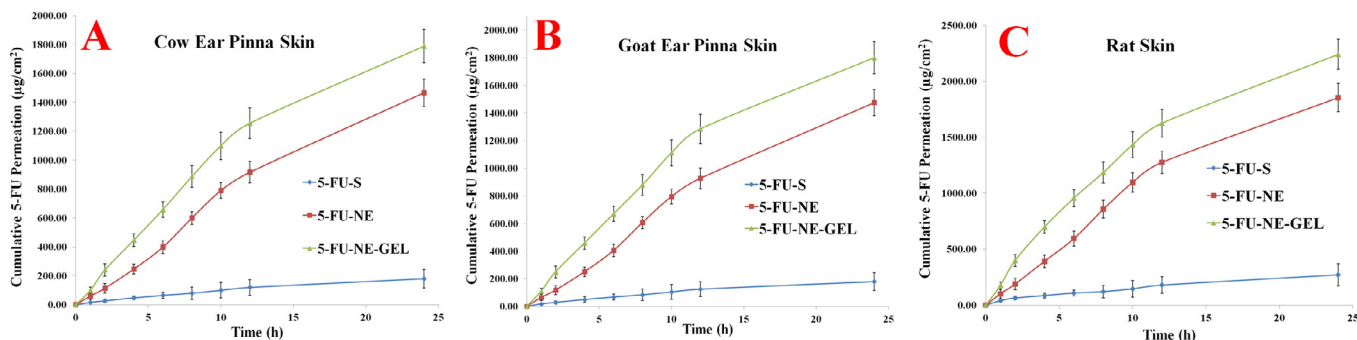


Fig. 7. showed a comparative ex vivo various skins (cow, goat, & rat) permeation study of 5-FU from 5-FU-NE and 5-FU-NE-Gel.

Table 3
Permeability Parameters of 5-FU on different animal skin (cow, goat, and rat).

Skin Model	Steady-state flux (J_{ss}) ($\mu\text{g}/\text{cm}^2/\text{h}$)			Permeability coefficient (K_p) ($\mu\text{g} \times 10^{-2}$)			Enhancement Ratio (Er)		
	5-FU-S (Control)	5-FU-NE	5-FU-NE-Gel	5-FU-S (Control)	5-FU-NE	5-FU-NE-Gel	5-FU-S (Control)	5-FU-NE	5-FU-NE-Gel
Cow Skin	0.957 ± 0.41	8.174 ± 0.63	9.851 ± 0.84	0.0957 ± 0.003	0.8174 ± 0.012	0.9851 ± 0.016	–	8.54	10.29
Goat Skin	0.957 ± 0.40	8.212 ± 0.64	9.895 ± 0.85	0.0957 ± 0.003	0.8212 ± 0.013	0.9895 ± 0.018	–	8.58	10.34
Rat Skin	1.350 ± 0.55	10.345 ± 0.97	12.0244 ± 1.12	0.1350 ± 0.007	1.0345 ± 0.061	1.2024 ± 0.073	–	7.66	8.91

viable skins. 5-FU is highly permeable for 5-FU-NE3-Gel for the cow skin model in place of retention in the skin. The retention of 5-FU evaluated into the SC and viable part of the various skins after 24.0 h (Fig. 11). On the basis of permeation results, we observed that highest amount of 5-FU collected in the viable part of the cow and goat skin model from 5-FU-NE3-Gel as compared to other preparations i.e., 5-FU-S and 5-FU-NE3 for rat skin model.

3.8. UHPLC-MS/MS data analysis for 5-FU

The analytical method was developed and validated displayed in Fig. 8 (MS spectra-scans of 5-FU), whereas representative chromatogram of 5-FU shown in Fig. 8C correspond with the retention time 1.710 min. Detailed description about in-house developed this method and their validation has been communicated into the another journal. Retention times of 0.736 and 2.185 min were observed for DDTC and 5-FU-DDTC complex, respectively (Fig. 10C). Preparation of reference standards have mentioned above in materials and methods. Mass spectrum of Diethyldithiocarbamate (DDTC)-MS-Scan and Sodium-Diethyldithiocarbamate (DDTC)-MS-Scan showed at protonated precursor $[M-H]^-$ ions at m/z 147.27, and 170.21 [Fig. 10A]. After the producing the coordination complex reaction, it showed the MS-Scan of complex 5-FU with Diethyldithiocarbamate (DDTC)-MS-Scan and Sodium-Diethyldithiocarbamate (DDTC)-MS-Scan product ion at m/z 277.09 and 300.26 [Fig. 10B]. This mass spectra has been explained it's self, the DDTC-5-FU coordination complex formed (Fig. 9). In Fig. 9, 5-Fluorouracil formed two isomers keto (amide) and enol (imide) form by the process of tautomerism. 5-fluorouracil in enol (imide) ionization takes place and formation a coordination complex with sodium Diethyldithiocarbamate (m/z 300.26 in negative ion mode i.e. for molecular formula $C_9H_{13}FN_3O_2S_2Na$). Mass spectra was also showed m/z i.e. 277.09, it means, this mass is without the sodium. Therefore, this mass spectra (Fig. 10B) showed two major mass peaks i.e. 277.09 is for $C_9H_{13}FN_3O_2S_2$ without the

sodium and other one was m/z 300.26 is due to the formation of 5-FU- coordination complex with sodium.

3.9. Stability studies on 5-FU-NE3

For stability studies, 5-FU-NE3 was chosen on the basis of smallest lowest globule size, smallest viscosity and maximum rate permeation in the different skin. Optimized 5-FU-NE3 nanoformulation characterized by viscosity, PDI, ZP, globule size, and RI for 3-months at 4.0 °C in the refrigerator temperature. There was no change in the viscosity, PDI, ZP, globule size, and RI was seen after storage in the 4.0 °C refrigerator temperature (Table 4). The globule size and PDI were determined 68.09 ± 2.61 nm and 0.226 ± 0.028 after storage of 90 days. Though, ZP, RI, and were found to be 53.16 ± 3.28 cps, 1.381 ± 0.023 and -22.29 mV after storage of 90 days (Table 4). Optimized-5-FU-NE3 was satisfactorily stable at refrigerator temperature as we found that no significant changes by physicochemical parameters.

3.10. Ex vivo vesicle-skin interaction studies by fluorescence microscopy

5-FU-S, 5-FU-NE3 & 5-FU-NE3-Gel tested on the CGR-skins on the basis of visualization of 6-carboxyfluorescein hydrophilic dye. 5-FU-NE3-Gel were analysed as based on fluorescence that showed the highly intensified results in the inter-corneocytes spaces (Fig. 12). These results may be due to the colloidal semisolid nanoformulations which were identified and given us a localized and controlled drug delivery and also working as a 5-FU reservoir. We have analysed the morphology of the skin at the time of permeation studies (before & after). We observed the little bit alteration in the CGR-skins that showed the more microporous studies after permeation studies (Figures are not shown).

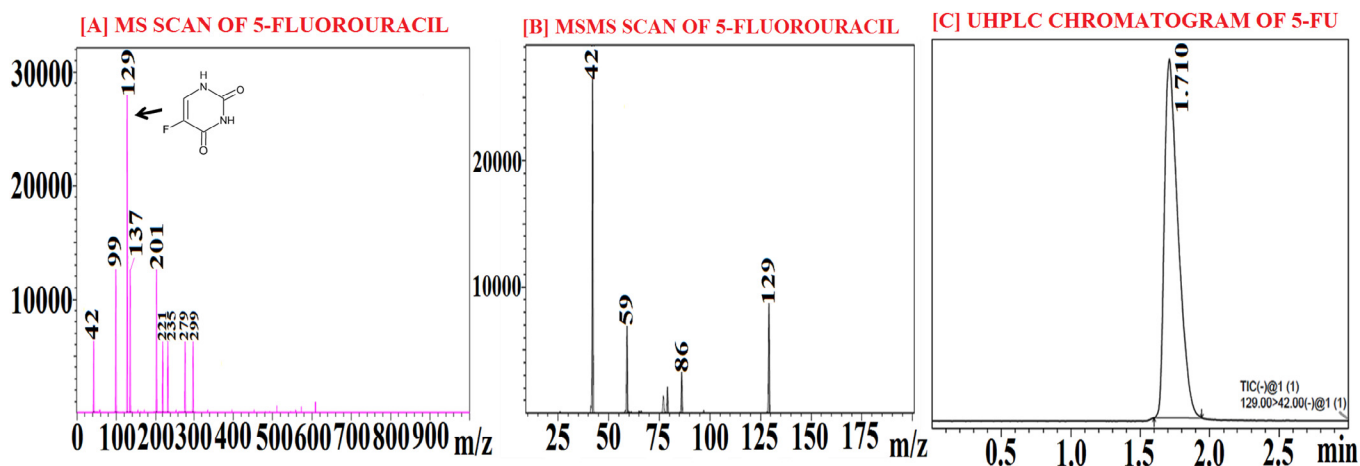


Fig. 8. Mass spectrum of 5-FU-MS-Scan i.e. protonated precursor $[M-H]^-$ ions at m/z 129 [A], 5-FU-MSMS-Scan fragmentation transitions i.e. major fragmented product ion at m/z 42 [B], and a chromatogram of UHPLC showing retention time 1.710 min.

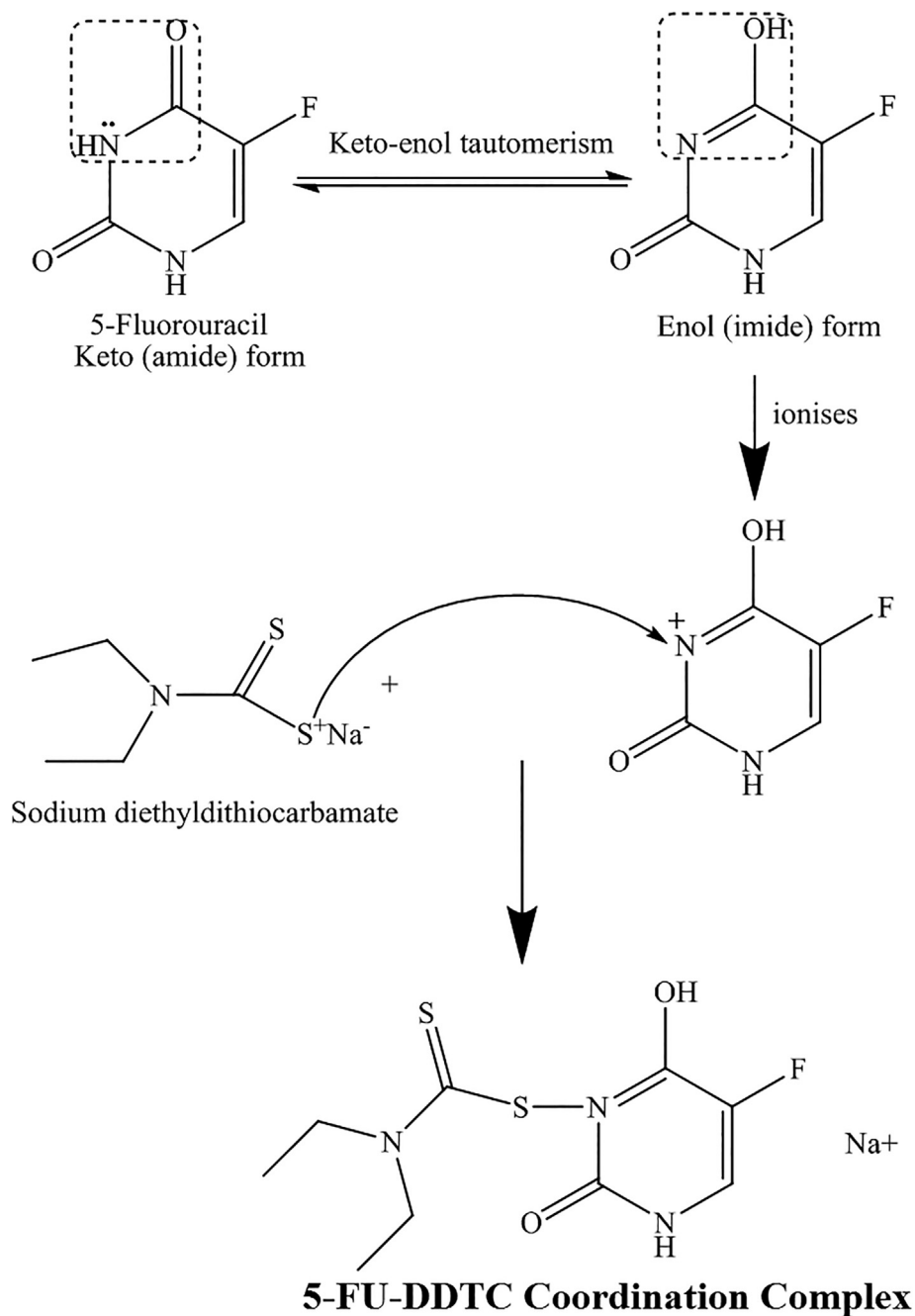


Fig. 9. 5-FU-DDTC complex formation by Keto-enol mechanism.

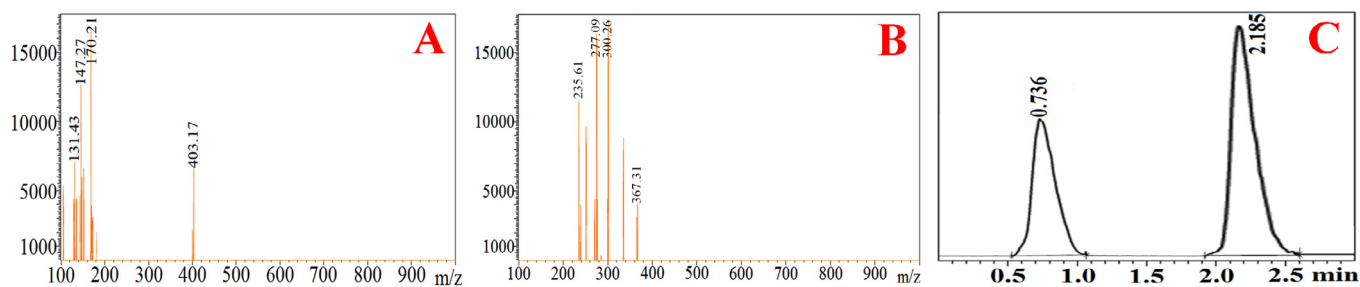


Fig. 10. Mass spectrum of Diethyldithiocarbamate (DDTC)-MS-Scan and Sodium-Diethyldithiocarbamate (DDTC)-MS-Scan showed at protonated precursor $[M-H]^-$ ions at m/z 147.27, and 170.21 [A], MS-Scan of complex 5-FU with Diethyldithiocarbamate (DDTC)-MS-Scan and Sodium-Diethyldithiocarbamate (DDTC)-MS-Scan product ion at m/z 277.09 and 300.26 [B], and a UHPLC chromatogram of showing retention time 0.736 and 2.185 min for DDTC chelating agent individual and DDTC-5-FU complex [C].

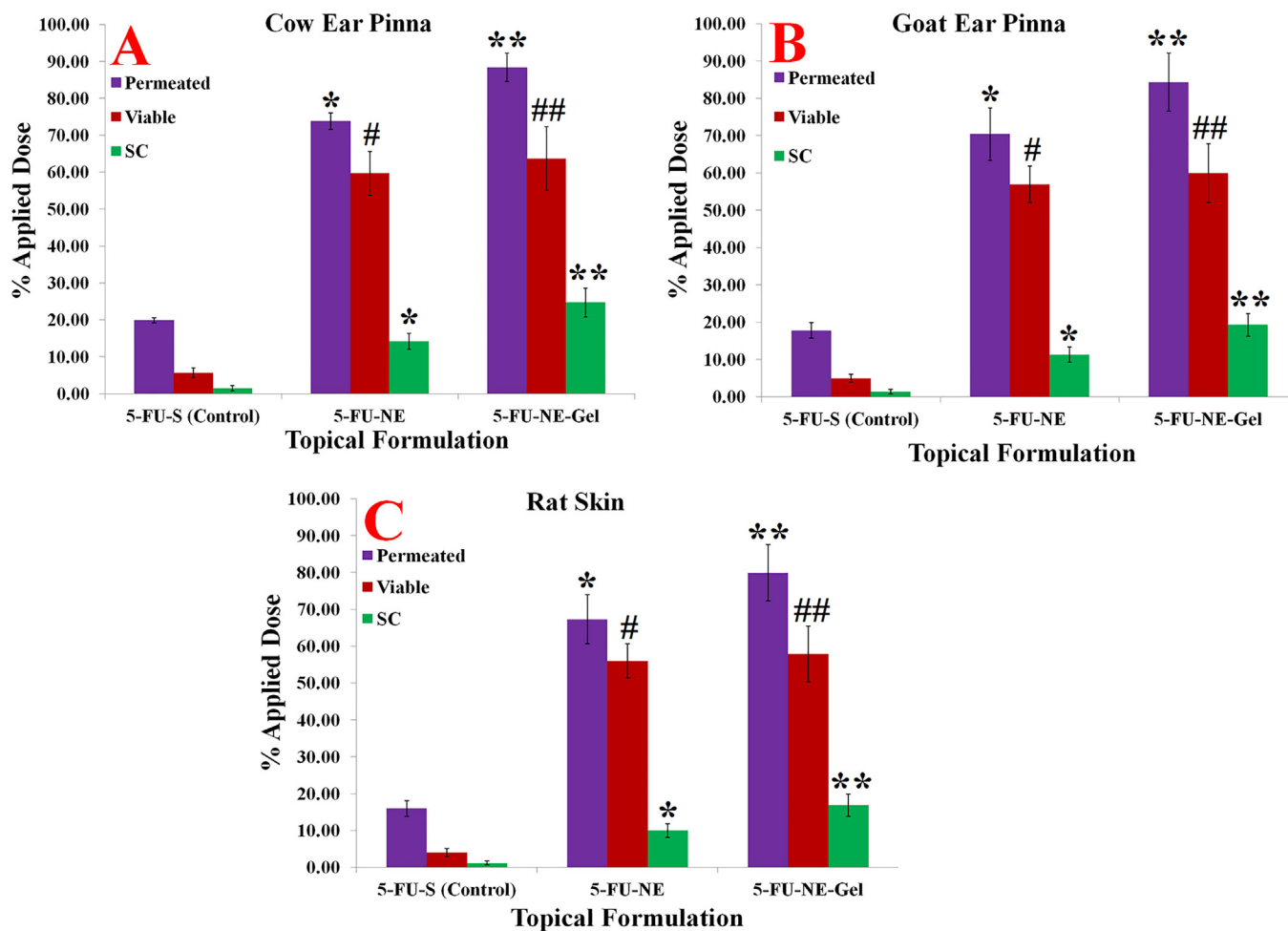


Fig. 11. %Age permeation of 5-FU and their retention of skin in stratum corneum (SC) and viable part of the skin *ex-vivo* from 5-FU, 5-FU-NE, and 5-FU-NE-Gel nanoformulation.

Table 4
Stability studies on 5-FU-NE3 in terms of physicochemical parameters at refrigerator temperature.

Time (Days)	Globule size \pm SD (nm)	PDI	Zeta Potential (mV)	RI \pm SD	Viscosity \pm SD (cps)	% Transmittance
0	66.97 \pm 2.46	0.216 \pm 0.020	-21.63	1.362 \pm 0.012	52.31 \pm 2.98	99.54 \pm 0.04
30	67.09 \pm 2.50	0.218 \pm 0.021	-21.98	1.370 \pm 0.016	52.91 \pm 3.29	99.03 \pm 0.05
60	67.54 \pm 2.56	0.221 \pm 0.024	-22.23	1.377 \pm 0.019	53.01 \pm 3.20	98.99 \pm 0.08
90	68.09 \pm 2.61	0.226 \pm 0.028	-22.29	1.381 \pm 0.023	53.16 \pm 3.28	98.80 \pm 0.05

3.11. *In vitro* cell lines studies for opt-5-FU-NE-Gel

5-FU-NE3 & 5-FU-NE3-Gel has been developed for the skin cancer chemoprevention. Both optimized-5-FU-NE3 & 5-FU-NE3-Gel have used to evaluate the *in vitro* therapeutic efficacy on the melanoma cancer cell lines (SK-MEL-5 type). Various molar concentrations of 5-FU from 5-FU-S, 5-FU-NE3 & 5-FU-NE3-Gel were used to evaluate *in vitro* cytotoxicity (%) by the melanoma cell lines. Different molar concentrations (3.2, 6.4, 12.8, 25.6, 51.2, and 102.4 μ M) of 5-FU in free 5-FU-S, 5-FU-NE3, and 5-FU-NE3-Gel were also used to evaluate Cell survival (%) (Fig. 13). Free 5-FU-S showed no significant cell inhibition on melanoma cell lines (Fig. 13). The %age cytotoxicity was observed i.e. 4.98 ± 0.41 at concentration of 102.4 μ M (Table 5). Though, 102.4 μ M 5-FU same concentration in optimized-5-FU-NE3, and 5-FU-NE3-Gel showed $61.75 \pm 4.38\%$ and $79.22 \pm 5.04\%$ cytotoxicity that was highly significant than free

5-FU-S ($p < 0.05$ & $p < 0.01$, respectively). 5-FU in the form of optimized-5-FU-NE3, and 5-FU-NE3-Gel were observed strongly effective and efficient than 5-FU-S on melanoma cell lines. Therefore, it means the highly potent therapeutic effectiveness of optimized-5-FU-NE3, and 5-FU-NE3-Gel for treatment of skin cancer. On the other side, the incubation of SK-MEL-5 cells with Placebo-nanoformulation (i.e. control, blank without 5-FU, NE-Gel) showed that not inhibit cells growth at better amount/numbers as represented in Fig. 13. Blank NE-Gel (control) showed negligible inhibition in the growth of cell that means no toxicity of optimized-NE-Gel. Optimized-5-FU-NE3-Gel was showed anticancer effects in the form cytotoxic effects due to the presence of 5-FU in 5-FU-NE3-Gel. 5-FU-NE3-Gel concentration showed 50% cell death (IC₅₀) that has been measured through concentration dependent cell viability curve (Fig. 13). 5-FU-S has not showed any value for IC₅₀ at predetermined concentrations due to absence

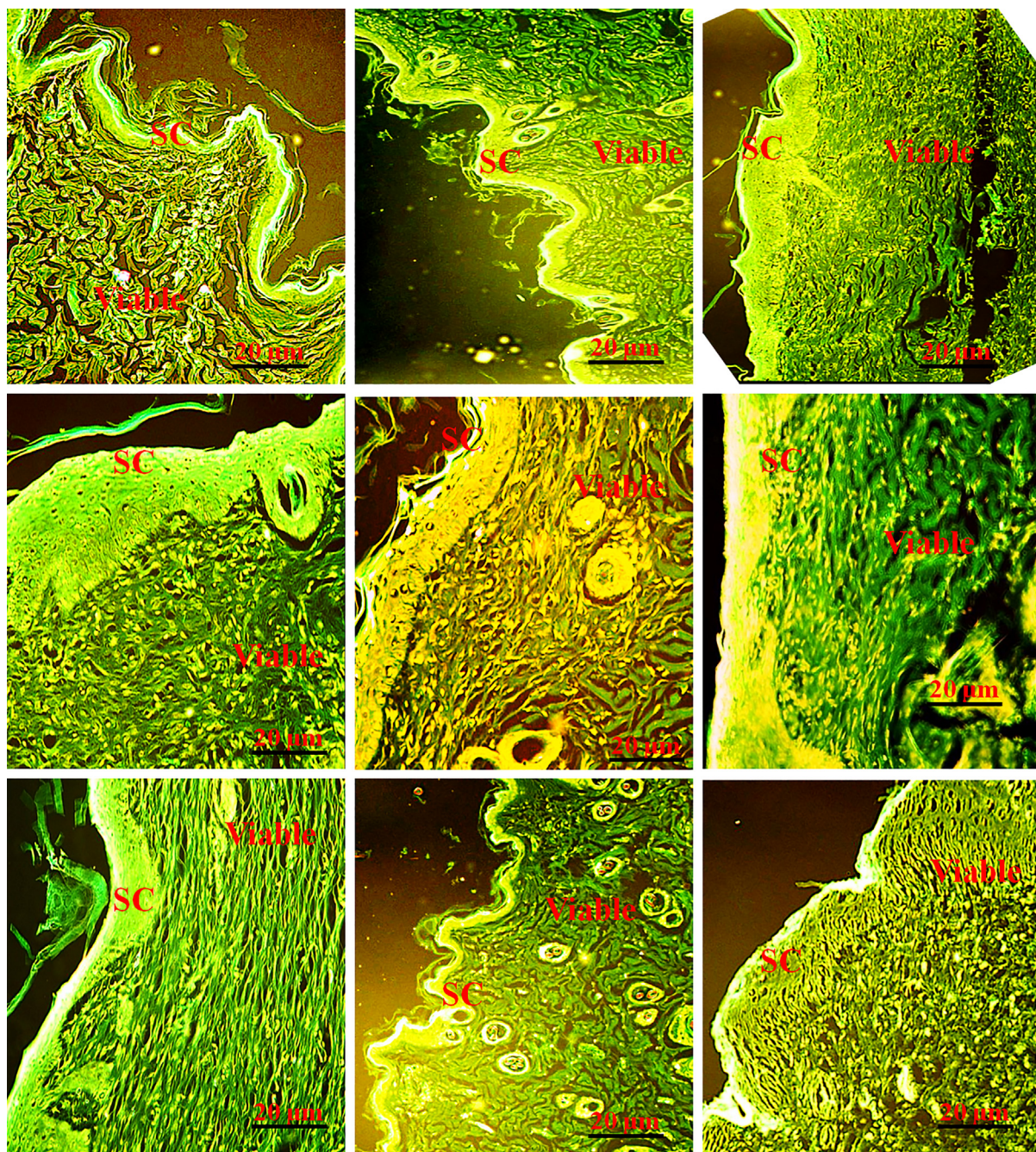


Fig. 12. Fluorescence micrographs of cow- and goat-ear pinna skin and rat skin treated with the formulation 5-FU-S (A) 5-FU-NE (B) 5-FU-NE-Gel (C). Different type of formulations labelled with hydrophilic fluorescence probe (6-carboxyfluorescein) to mark the penetration of the 5-FU to deep skin strata.

or negligible results of cell growth inhibition from the 5-FU-S. On the other side, 5-FU IC₅₀ value from the 5-FU-NE3-Gel showed i.e. 12.9 µM (Table 5). On the basis of IC₅₀ value, the 5-FU in 5-FU-NE3-Gel was observed highly efficacious than 5-FU-S that decrement of the 5-FU dose with adverse effects of 5-FU related with its oral drug delivery. Finally concluded, on the basis of observed results 5-FU-NE3-Gel showed could be effectively utilized topically as treatment of skin cancer.

Carbopol gel based 5-FU-NE3-Gel system can be responsible for the rate-limiting effect in the permeation of 5-FU from 5-FU-NE3-Gel. 5-FU-NE3-Gel absorbs water due to the presence of Carbopol that are linked with the relaxation of polymer chain and it was

already entrapped inside the 5-FU-NE3 as proved by the DSC and ATR data in which gel offer the intramatrix space and sustained form through 5-FU released in a controlled manner over a long period of time. This is a best correlation in terms of permeation parameters between cow and goat skin model when it compared to rat skin model. It can be good similarities of skins based on structural and anatomical morphology of cow and goat skins. Additionally, it is very difficult to perform our research experiments on human skin. On the basis of previously reported literature (Gupta and Trivedi, 2015; Jangdey et al., 2017; Pradhan et al., 2015; Biswas et al., 2016), the cow and goats skins are contained both epidermis and dermis with their characteristics features same like

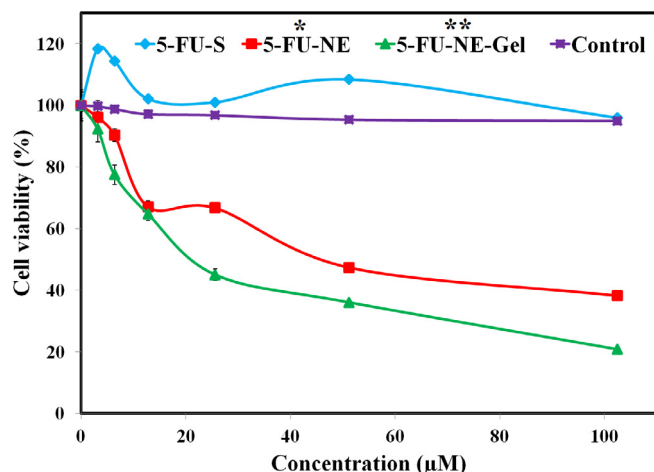


Fig. 13. %Age-Cell viability (n = 3, SD, mean) of 5-FU in free 5-FU aqueous solution, control, and optimized-5-FU-NE, and 5-FU-NE-Gel nanoformulation on melanoma cell lines. Optimized-5-FU-NE3 (p < 0.05) and 5-FU-NE3-Gel (p < 0.01) were highly significant than free 5-FU-S.

human skins. The skin of laboratory animals, for example, rat, mice, rabbits, guinea pigs etc. shows marked anatomic differences from human skin. Moreover, the skins of rats, mice, guinea pigs, rabbits etc., already showed the anatomic variability to the human skin. These mentioned animals exhibited very thin epidermis and the flat epidermal–dermal interface that does not contain ridges and papillary projections. It is very difficult to obtain an ethical approval for human skins and primate research. Therefore, we selected the cow and goat skins. These skins showed very close to human skins as per the morphologically and functionally reported data (Jangdey et al., 2017; Pradhan et al., 2015; Biswas et al., 2016; Calabrese 1984, Monteiro-Riviere and Riviere 1996).

Moreover, they lose dermal structures as comparatively human skin and also showed under-developed. Hence, most of the animal's skins showed a much weaker barrier as compared to the human skin. The retention of 5-FU enhanced from the 5-FU-NE3-Gel in SC and viable part of the skin exhibits the efficiency of the 5-FU-NE3-Gel prepared with the carbopol-940 gel base using with Transcutol HP and PEG-400 (Prasanthi and Lakshmi, 2012; Junyaprasert et al., 2013; Dubey et al., 2017).

A very high deposition of fluorescence probe in the deep skin layer from 5-FU-NE3-Gel can be believed due to the presence of carbopol. A cross-linked polymer i.e. carbopol formed a matrix-type reservoir at the time of gel formulation and their release of 5-FU slowly for an extended over the time period (Han et al., 2012). Entrapment of the lipid vesicles showed an intra-matrix system formed by carbopol gel which is responsible for the deposition of 5-FU/any drug in the deep skin layer. Carbopol based gel

i.e. 5-FU-NE3-Gel was showed the results that increased the retention of 5-FU inside the skin. Therefore, it provided much more and controlled skin extent of 5-FU without any increasing the systemic absorption of 5-FU. These characteristic functional groups from the all absorption spectrum showed within the range. Therefore, 5-FU and all excipients are compatible to each other.

In general, the cytotoxicity is the most important test to evaluate the biocompatibility. Novel optimized nanoformulations (5-FU-NE3 and 5-FU-NE3-Gel) have been examined through *in vitro* methods and also to evade unnecessary sacrificing the animals. A novel 5-FU-NE-Gel is also evaluated for the cytotoxicity study i.e. the first-level examination prior to its application on biomedical processes. All the results signified enhances the lethality with the enhancement of 5-FU concentrations that indicates that it is a dose dependent effect. 5-FU-NE3-Gel enhanced the cytotoxicity by the increment of 5-FU cellular uptake by a novel 5-FU-NE3-Gel by the pathway of endocytosis that can be characteristic by targeted 5-FU delivery systems commonly. Hence we concluded that a very high amount of 5-FU concentration can be delivered inside the tumor cells via targeted drug delivery system. Thus, it is a best cytotoxic effects promotion (Ahmad et al., 2019e; Mangalathillam et al., 2012).

4. Conclusion

A nanoemulsion (5-FU-NE) has been optimized containing aqueous phase (including 10.0 mg 5-FU; 20.0% w/w); Transcutol-HP (27.0% w/w), PEG-400 (13.0% w/w) and Castor oil (40% w/w) on basis of smallest globule size, smallest PDI, optimum viscosity, optimized concentration of oil. After the conversion of 5-FU-NE into gel by the Carbopol 934, we found and compared the DSC, FT-IR, Release, and permeation results showed the highest and optimum accepted outcome with 5-FU-NE-Gel in comparison of 5-FU-NE for the further research studies. As per, 5-FU permeation and their localization of cow skin were quantitatively same as goat skin but it differ from rat skin. On the basis of results, localization of 5-FU from the 5-FU-NE-Gel was maximum quantity as compared to other two formulations in the viable skin and it was also observed less permeation which imitates the decreased in the systemic toxicity of 5-FU. Additionally, 5-FU-loaded-NE-gel improved the delivery of 5-FU to treat skin-cited melanoma cancer cells on the basis of *in vitro* cell lysis results. Optimized-5-FU-NE3-Gel showed the higher efficacy than 5-FU-S on the melanoma cancer cells as per the results of *in vitro* cytotoxicity assay. Finally, it is concluded that optimized-5-FU-NE3-Gel could be a great tool for the treatment and their chemoprevention of skin cancer. Although, all the data should be needed to examine human skin permeation data with the abnormal skin to develop a risk versus benefit ratio. Moreover, these data should be confirmed on the basis of preclinical and clinical studies.

Table 5

IC50 and % Cytotoxicity of free 5-FU, opt-5-FU-NE, 5-FU-NE-Gel, and control on melanoma cancer cell lines (n = 3).

Concentration (µM)	Cell Death (% ±SD)				IC50			
	5-FU-S	5-FU-NE	5-FU-NE-Gel	Control (NE-Gel: Placebo)	5-FU	5-FU-NE	5-FU-NE-Gel	Control (NE-Gel: Placebo)
0	0	0	0	0				
3.2	-18.38 ± 0.93	3.92 ± 0.17	7.78 ± 0.87	0.28 ± 0.00				
6.4	-14.31 ± 0.79	9.61 ± 1.02	22.51 ± 1.82	1.17 ± 0.09				
12.8	-2.13 ± 0.21	32.94 ± 1.96	35.29 ± 2.07	2.81 ± 1.21	NI	25.3	12.9	-
25.6	1.03 ± 0.18	33.27 ± 2.09	54.97 ± 3.13	3.16 ± 1.29				
51.2	-8.41 ± 0.88	52.62 ± 2.97	63.97 ± 4.14	4.61 ± 1.87				
102.4	4.98 ± 0.41	61.75 ± 4.38	79.22 ± 5.04	5.01 ± 1.91				

Not Identified (NI), The concentration at which 50% cell death (IC50).

Declaration of Competing Interest

The authors declare that they have no known competing financial interests or personal relationships that could have appeared to influence the work reported in this paper.

Acknowledgments

The authors are very thankful to Animal House, Institute for Research and Medical Consultations (IRMC), Imam Abdulrahman Bin Faisal University, Dammam, Kingdom of Saudi Arabia.

References

- Ahmad, N., Alam, M.A., Ahmad, F.J., Sarafroz, M., Ansari, K., Sharma, S., Amir, M., 2018a. Ultrasonication Techniques used for the preparation of novel Eugenol-Nanoemulsion in the treatment of wounds healings and anti-inflammatory. *J. Drug Deliv. Sci. Technol.* 46, 461–473. <https://doi.org/10.1016/j.jddst.2018.06.003>.
- Ahmad, N., Ahmad, R., Alam, M.A., Ahmad, F.J., Amir, M., 2018b. Impact of ultrasonication techniques on the preparation of novel Amiloride-nanoemulsion used for intranasal delivery in the treatment of epilepsy. *Artif. Cells Nanomed. Biotechnol.* 46 (sup3), S192–S207. <https://doi.org/10.1080/21691401.2018.1489826>.
- Ahmad, N., Ahmad, R., Naqvi, A.A., Alam, M.A., Ashafaq, M., Rub, R.A., Ahmad, F.J., 2018c. Intranasal delivery of quercetin-loaded mucoadhesive nanoemulsion for treatment of cerebral ischaemia. *Artif. Cells Nanomed. Biotechnol.* 46 (4), 717–729. <https://doi.org/10.1080/21691401.2017.1337024>.
- Ahmad, N., Alam, M.A., Ahmad, R., Umar, S., Ahmad, F.J., 2018d. Improvement of oral efficacy of Irinotecan through biodegradable polymeric nanoparticles through in vitro and in vivo investigations. *J. Microencapsul.* 35 (4), 327–343. <https://doi.org/10.1080/02652048.2018.1485755>.
- Ahmad, N., Ahmad, R., Al-Qudaihi, A., Alaseel, S.E., Fita, I.Z., Khalid, M.S., Pottoo, F.H., Bolla, S.R., 2019a. A novel self-nanoemulsifying drug delivery system for curcumin used in the treatment of wound healing and inflammation. *3 Biotech* 9 (10). <https://doi.org/10.1007/s13205-019-1885-3>.
- Ahmad, N., Ahmad, R., Al-Qudaihi, A., Alaseel, S.A., Fita, I.Z., Khalid, M.S., Pottoo, F.H., 2019b. Preparation of a novel curcumin nanoemulsion by ultrasonication and its comparative effects in wound healing and the treatment of inflammation. *RSC Advances*. 9, 20192–20206. <https://doi.org/10.1039/C9RA03102B>.
- Ahmad, N., Ahmad, F.J., Bedi, S., Sharma, S., Umar, S., Ansari, M.A., 2019c. A novel nanoformulation development of Eugenol and their treatment in inflammation and periodontitis. *Saudi Pharm. J.* 27 (6), 778–790. <https://doi.org/10.1016/j.jsps.2019.04.014>.
- Ahmad, N., Al-Subaiee, A.M., Ahmad, R., Sharma, S., Alam, M.A., Ashafaq, M., Abdur Rub, R., Ahmad, F.J., 2019d. Brain-targeted glycyrrhizic-acid-loaded surface decorated nanoparticles for treatment of cerebral ischaemia and its toxicity assessment. *Artif Cells Nanomed. Biotechnol.* 47 (1), 475–490. <https://doi.org/10.1080/21691401.2018.1561458>.
- Ahmad, N., Ahmad, R., Alam, M.A., Ahmad, F.J., Amir, M., Pottoo, F.H., Sarafroz, M., Jafar, M., Umar, K., 2019e. Daunorubicin oral bioavailability enhancement by surface coated natural biodegradable macromolecule chitosan based polymeric nanoparticles. *Int. J. Biol. Macromol.* 128, 825–838. <https://doi.org/10.1016/j.ijbiomac.2019.01.142>.
- ElMeshad, I., Ibrahim, M.T., 2011. Transdermal delivery of an anti-cancer drug via W/O emulsions based on alkyl polyglycosides and lecithin: design, characterization, and in vivo evaluation of the possible irritation potential in rats. *AAPS PharmSciTech.* 12 (1), 1–9. <https://doi.org/10.1208/s12249-010-9557-y>.
- Alvi, I.A., Madan, J., Kaushik, D., Sardana, S., Pandey, R.S., Ali, A., 2011. Comparative study of transferosomes, liposomes, and nisomes for topical delivery of 5-fluorouracil to skin cancer cells: preparation, characterization, in vitro release, and cytotoxicity analysis. *Anticancer Drugs.* 22 (8), 774–782. <https://doi.org/10.1097/CAD.0b013e328346c7d6>.
- Ammar, H.O., Salama, H.A., Ghorab, M., Mahmoud, A.A., 2009. Nanoemulsion as a potential ophthalmic drug delivery system for dorzolamide hydrochloride. *AAPS Pharm. Sci. Tech.* 10 (3), 808–819. <https://doi.org/10.1208/s12249-009-9268-4>.
- Bhattacharjee, S., 2016. DLS and zeta potential—what they are and what they are not? *J. Control Release* 235, 337–351. <https://doi.org/10.1016/j.jconrel.2016.06.017>.
- Biswas, G.R., Majee, S.B., Roy, A., 2016. Combination of synthetic and natural polymers in hydrogel: An impact on drug permeation. *J. Appl. Pharm. Sc.* 6 (11), 158–164. <https://doi.org/10.7324/JAPS.2016.601125>.
- Bronaugh, R.L., Stewart, R.F., Congdon, E.R., 1982. Methods for *in vitro* percutaneous absorption studies II. Animal models for human skin. *Toxicol. Appl. Pharmacol.* 62, 481–488. [https://doi.org/10.1016/0041-008X\(82\)90149-1](https://doi.org/10.1016/0041-008X(82)90149-1).
- Bronaugh, R.L., Stewart, R.F., 1985. Methods for *in vitro* percutaneous absorption studies IV: The flow-through diffusion cell. *J. Pharm. Sci.* 74, 64–67. <https://doi.org/10.1002/jps.2600740117>.
- Calabrese, E.J., 1984. Gastrointestinal and dermal absorption: interspecies differences. *Drug Metab. Rev.* 15, 1013–1032. <https://doi.org/10.3109/03602538409033556>.
- Chauhan, A., Zubair, S., Sherwani, A., Owais, M., 2012. Aloe vera induced bimimetic assemblage of nucleobase into nanosized particles. *Plos One* 7 (3), E32049. <https://doi.org/10.1371/journal.pone.0032049>.
- Cosco, D., Paolino, D., Muzzalupo, R., Celia, C., Citraro, R., Caponio, D., Picci, N., Fresta, M., 2009. Novel PEG-coated nisomes based on bola-surfactant as drug carriers for 5-fluorouracil. *Biomed. Microd.* 11 (5), 1115–1125. <https://doi.org/10.1007/s10544-009-9328-2>.
- Craig, D.Q.M., Barker, S.A., Banning, D., 1995. An investigation into the mechanisms of self-emulsification using particle size analysis and low frequency dielectric spectroscopy. *Int. J. Pharm.* 114 (1), 103–110. [https://doi.org/10.1016/0378-5173\(94\)00222-Q](https://doi.org/10.1016/0378-5173(94)00222-Q).
- Dubey, S., Sharma, R., Mody, N., Vyas, S.P., 2017. Novel carriers and approaches: insight for psoriasis management. nanostructures for novel therapy synthesis, characterization and applications micro and nano technologies. (Chapter 24), 657–684.
- Elmaghraby, G.M., 2008. Transdermal delivery of hydrocortisone from eucalyptus oil microemulsion: effects of cosurfactants. *Int. J. Pharm.* 355 (1–2), 285–292. <https://doi.org/10.1016/j.ijpharm.2007.12.022>.
- Elmeshad, A.N., Tadros, M.I., 2011. Transdermal delivery of an anticancer drug via w/o emulsions based on alkyl polyglycosides and lecithin: design, characterization and in vivo evaluation of the possible irritation potential in rats. *AAPS Pharm. Sci. Tech.* 12 (1), 1–9. <https://doi.org/10.1208/s12249-010-9557-y>.
- Fang, J.Y., Hung, C.F., Fang, Y.P., Chan, T.F., 2004. Transdermal iontophoresis of 5-fluorouracil combined with electroporation and laser treatment. *Int. J. Pharm.* 270 (1–2), 241–249. <https://doi.org/10.1016/j.ijpharm.2003.10.025>.
- Gupta, R.R., Jain, S.K., Varshney, M., 2005. AOT water-in-oil microemulsions as a penetration enhancer in transdermal drug delivery of fluorouracil. *Coll. Surf. B.* 41 (1), 25–32. <https://doi.org/10.1016/j.colsurfb.2004.09.008>.
- Gupta, V., Trivedi, P., 2015. *Ex vivo* localization and permeation of cisplatin from novel topical formulations through excised pig, goat, and mice skin and in vitro characterization for effective management of skin-cited malignancies. *Artif. Cells Nanomed. Biotechnol.* 43 (6), 373–382. <https://doi.org/10.3109/21691401.2014.893523>.
- Han, F., Yin, R., Che, X., Yuan, J., Cui, Y., Yin, H., Li, S., 2012. Nanostructured lipid carriers (NLC) based topical gel of flurbiprofen: design, characterization and in vivo evaluation. *Int. J. Pharm.* 439 (1–2), 349–357. <https://doi.org/10.1016/j.ijpharm.2012.08.040>.
- Hwangl, T.L., Fang, C.L., Chen, C.H., Fang, J.Y., 2009. Permeation enhancer containing water-in-oil nanoemulsions as carriers for intravesical cisplatin delivery. *Pharm. Res.* 26 (10), 2314–2323. <https://doi.org/10.1007/s11095-009-9947-6>.
- Jangdey, M.S., Gupta, A., Saraf, S., 2017. Fabrication, in-vitro characterization, and enhanced in-vivo evaluation of carbopol-based nanoemulsion gel of apigenin for UV-induced skin carcinoma. *Drug Deliv.* 24 (1), 1026–1036. <https://doi.org/10.1080/10717544.2017.1344333>.
- Junyaprasert, V.B., Singhsa, P., Jintapattanakit, A., 2013. Influence of chemical penetration enhancers on skin permeability of ellagic acid-loaded nisomes. *Asian J. Pharm. Sci.* 8 (2), 110–117. <https://doi.org/10.1016/j.ajps.2013.07.014>.
- Khan, G.M., Hussain, A., Hanif, R.M., 2011. Preparation and evaluation of 5,9 dimethyl-2-cyclopropyl-2-decanol as a penetration enhancer for drugs through rat skin. *Pak. J. Pharm. Sci.* 24 (4), 451–457.
- Khandavilli, S., Panchagnula, R., 2007. Nanoemulsions as versatile formulations for paclitaxel delivery: peroral and dermal delivery studies in rats. *J. Invest. Dermatol.* 127 (1), 154–162. <https://doi.org/10.1038/sj.jid.5700485>.
- Kong, M., Chen, X.G., Kwon, D.K., Park, H.J., 2011. Investigations on skin permeation of hyaluronic acid based nanoemulsions as transdermal carrier. *Carbohydr. Polym.* 86 (2), 837–843. <https://doi.org/10.1038/sj.jid.5700485>.
- Kotta, S., Khan, A.W., Ansari, S.H., Sharma, R.K., Ali, J., 2015. Formulation of nanoemulsion: a comparison between phase inversion composition method and high-pressure homogenization method. *Drug Deliv.* 22 (4), 455–466. <https://doi.org/10.3109/10717544.2013.866992>.
- Lawrence, M.J., Rees, G.D., 2000. Microemulsion-based media as novel drug delivery systems. *Adv. Drug Deliv. Rev.* 45 (1), 89–121. [https://doi.org/10.1016/S0169-409X\(00\)0103-4](https://doi.org/10.1016/S0169-409X(00)0103-4).
- Liu, F., Xiao, Y.Y., Ping, Q.N., Yang, C., 2009. Water in oil microemulsions for transdermal delivery of fluorouracil. *Yao Xue Xue Bao.* 44 (5), 540–547.
- Mangalathillam, S., Rejinold, N.S., Nair, A., Lakshmanan, V.K., Nair, S.V., Jayakumar, R., 2012. Curcumin loaded chitin nanogels for skin cancer treatment via the transdermal route. *Nanoscale.* 4 (1), 239–250. <https://doi.org/10.1039/C1NR11271F>.
- Meidan, V.M., Walmsley, A.D., Docker, M.F., Irwin, W.J., 1999. Ultrasoundenhanced diffusion into coupling gel during phonophoresis of 5-fluorouracil. *Int. J. Pharm.* 185, 205–213. [https://doi.org/10.1016/S0378-5173\(99\)00168-4](https://doi.org/10.1016/S0378-5173(99)00168-4).
- Monteiro-Riviere, N., Riviere, J.E., 1996. The pig as a model for cutaneous pharmacology and toxicology research. In: Tumbleson, M.E., Shook, L.B. (Eds.), *Advances in Swine in Biomedical Research*. Plenum Press, New York, pp. 425–458.

- Narkhede, R.S., Gujar, K.N., Gambhire, V.M., 2014. Design and evaluation of self-nanoemulsifying drug delivery systems for nebulolol hydrochloride. *Asian J. Pharm.* 8 (3), 200–209. <https://doi.org/10.4103/0973-8398.139190>.
- Panchagnula, R., Stemmer, K., Ritschel, W.A., 1997. Animal models for transdermal drug delivery methods and findings. *Methods Find. Exp. Clin. Pharmacol.* 19 (5), 335–341.
- Pouton, C.W., Porter, C.J., 2008. Formulation of lipid-based delivery systems for oral administration: materials, methods and strategies. *Adv. Drug Deliv. Rev.* 60 (6), 625–637. <https://doi.org/10.1016/j.addr.2007.10.010>.
- Pradhan, M., Singh, D., Murthy, S.N., Singh, M.R., 2015. Design, characterization and skin permeating potential of Fluocinolone acetonide loaded nanostructured lipid carriers for topical treatment of psoriasis. *Steroids*, 101, 56–63. <https://doi.org/10.1016/j.steroids.2015.05.012>.
- Prasanthi, D., Lakshmi, P.K., 2012. Effect of chemical enhancers in transdermal permeation of alfuzosin hydrochloride. *ISRN Pharm.* 2012., <https://doi.org/10.5402/2012/965280> 965280.
- Rajinikanth, P.S., Chellian, J., 2016. Development and evaluation of nanostructured lipid carrier-based hydrogel for topical delivery of 5-fluorouracil. *Int. J. Nanomed.* 11, 5067–5077. <https://doi.org/10.2147/IJN.S117511>.
- Saif, M.W., Choma, A., Salamone, S.J., Chu, E., 2009. Pharmacokinetically guided dose adjustment of 5-fluorouracil: a rational approach to improving therapeutic outcomes. *J. Natl. Cancer Inst.* 101 (22), 1543–1552. <https://doi.org/10.1093/jnci/djp328>.
- Sato, K., Sugibayashi, Y.M., 1991. Species differences in percutaneous absorption of nicorandil. *J. Pharm. Sci.* 80 (2), 104–107. <https://doi.org/10.1002/jps.2600800203>.
- Schmook, F.P., Meingassner, J.G., Billich, A., 2001. Comparison of human skin or epidermis models with human and animal skin in *in-vitro* percutaneous absorption. *Int. J. Pharm.* 215 (1–2), 51–56. [https://doi.org/10.1016/S0378-5173\(00\)00665-7](https://doi.org/10.1016/S0378-5173(00)00665-7).
- Shakeel, F., Ramadan, W., Ahmed, M.A., 2009. Investigation of true nanoemulsions for transdermal potential of indomethacin: characterization, rheological characteristics and *ex vivo* skin permeation studies. *J. Drug Target.* 17 (6), 435–441. <https://doi.org/10.1080/10611860902963021>.
- Shakeel, F., Ramadan, W., 2010. Transdermal delivery of anticancer drug caffeine from water-in-oil nanoemulsions. *Coll. Surf. B Biointerf.* 75 (1), 356–362. <https://doi.org/10.1016/j.colsurfb.2009.09.010>.
- Singh, B.N., Singh, R.B., Singh, J., 2005. Effects of ionization and penetration enhancers on the transdermal delivery of 5-fluorouracil through excised human stratum corneum. *Int. J. Pharm.* 298 (1), 98–107. <https://doi.org/10.1016/j.ijpharm.2005.04.004>.
- Singh, B.N., Jayaswal, S.B., 2008. Iontophoretic delivery of 5-fluorouracil through excised human stratum corneum. *Drug Discov. Ther.* 2 (2), 128–135.
- Sood, S., Jain, K., Gowthamarajan, K., 2014. Optimization of curcumin nanoemulsion for intranasal delivery using design of experiment and its toxicity assessment. *Coll. Surf. B Biointerf.* 113, 330–337. <https://doi.org/10.1016/j.colsurfb.2013.09.030>.
- Spermath, A., Aserin, A., Ziseran, L., Danino, D., Garti, N., 2007. Phosphatidylcholine embedded microemulsions: physical properties and improved Caco-2 cell permeability. *J. Controlled Release*. 119 (3), 279–290. <https://doi.org/10.1016/j.jconrel.2007.02.014>.
- Thomas, A.M., Kapanen, A.L., Hare, J.L., Ramsay, E., Edwards, K., Karlsson, G., Bally, M. B., 2011. Development of a liposomal nanoparticle formulation of 5-fluorouracil for parenteral administration: formulation design, pharmacokinetics and efficacy. *J. Controlled Release* 150 (2), 212–219. <https://doi.org/10.1016/j.jconrel.2010.11.018>.
- Tsuji, T., Sugai, T., 1983. Topically administered fluorouracil in vitiligo. *Arch. Dermatol.* 119 (9), 722–727. <https://doi.org/10.1001/archderm.1983.01650330014006>.
- Vallet, V., Cruz, C., Licausi, J., Bazire, A., Lallement, G., Boudry, I., 2008. Percutaneous penetration and distribution of VX using *in vitro* pig or human excised skin: Validation of demeton-S-methyl as adequate stimulant for VX skin permeation investigations. *Toxicology*. 246 (1), 73–82. <https://doi.org/10.1016/j.tox.2007.12.027>.
- van Ruth, S., Jansman, F.G., Sanders, C.J., 2006. Total body topical 5-fluorouracil for extensive non-melanoma skin cancer. *Pharm. World Sci.* 28 (3), 159–162. <https://doi.org/10.1007/s11096-006-9030-x>.
- Vecchia, B.E., Bunge, A., 2006. Animal models: a comparison of permeability coefficients for excised skin from humans and animals. In: Riviere, J.E. (Ed.), *The Dermal Absorption Models in Toxicology and Pharmacology*. CRC Press, Boca Raton, pp. 305–333.
- Gattu, S., Maibach, H.I., 2011. Modest but increased penetration through damaged skin: an overview of the *in vivo* human model. *Skin Pharmacol Physiol.* 24 (1), 2–9. <https://doi.org/10.1159/000314995>.
- Wan, S., Zhang, L., Quan, Y., Wei, K., 2018. Resveratrol-loaded PLGA nanoparticles: enhanced stability, solubility and bioactivity of resveratrol for non-alcoholic fatty liver disease therapy. *R. Soc. Open Sci.* 5, (11). <https://doi.org/10.1098/rsos.18145> 7 181457.
- Williams, A.C., 1971. Topical 5-FU—a new approach to skin cancer. *Ann Surg.* 173 (6), 864–871. <https://doi.org/10.1097/0000658-197106010-00003>.
- Zhang, Z., Wo, Y., Zhang, Y., Wang, D., He, R., Chen, H., Cui, D., 2012. *In vitro* study of ethosome penetration in human skin and hypertrophic scar tissue. *Nanomedicine* 8 (6), 1026–1033. <https://doi.org/10.1016/j.nano.2011.10.006>.
- Zhu, L., Ma, J., Jia, N., Zhao, Y., Shen, H., 2009. Chitosan coated magnetic nanoparticles as carriers of 5-fluorouracil: preparation, characterization and cytotoxicity studies. *Colloids Surf. B Biointerf.* 68 (1), 1–6. <https://doi.org/10.1016/j.colsurfb.2008.07.020>.